RECLAMATION

Managing Water in the West

Report DSO-06-03

Investigation of the Failure Modes of Concrete Dams Physical Model Tests

Dam Safety Technology Development Program

U.S. Department of the Interior
Bureau of Reclamation
Technical Service Center
Denver, Colorado

December 2006

REPORT DOCUMENTATION PAGE

Form Approved
OMB No. 0704-0188

The public reporting burden for this collection of information is estimated to average 1 hour per response, including the time for reviewing instructions, searching existing data sources, gathering and maintaining the data needed, and completing and reviewing the collection of information. Send comments regarding this burden estimate or any other aspect of this collection of information, including suggestions for reducing the burden, to Department of Defense, Washington Headquarters Services, Directorate for Information Operations and Reports (0704-0188), 1215 Jefferson Davis Highway, Suite 1204, Arlington, VA 22202-4302. Respondents should be aware that notwithstanding any other provision of law, no person shall be subject to any penalty for failing to comply with a collection of information if it does not display a currently valid OMB control number.

PLEASE DO NOT RETURN YOUR FORM TO THE ABOVE ADDRESS.

1. REPORT DATE *(DD-MM-YYYY)*	**2. REPORT TYPE**	**3. DATES COVERED** *(From - To)*
12-2006		

4. TITLE AND SUBTITLE
Investigation of the Failure Modes of Concrete Dams—Physical Model Tests

5a. CONTRACT NUMBER

5b. GRANT NUMBER

5c. PROGRAM ELEMENT NUMBER

6. AUTHOR(S)
Harris, David W. and Fred Travers

5d. PROJECT NUMBER

5e. TASK NUMBER

5f. WORK UNIT NUMBER

7. PERFORMING ORGANIZATION NAME(S) AND ADDRESS(ES)
Bureau of Reclamation
Technical Service Center
Materials Engineering and Research Laboratory
Denver, Colorado

8. PERFORMING ORGANIZATION REPORT NUMBER
DSO-06-03

9. SPONSORING/MONITORING AGENCY NAME(S) AND ADDRESS(ES)
Bureau of Reclamation
Denver, Colorado

10. SPONSOR/MONITOR'S ACRONYM(S)

11. SPONSOR/MONITOR'S REPORT NUMBER(S)
DSO-06-03

12. DISTRIBUTION/AVAILABILITY STATEMENT
National Technical Information Service, 5285 Port Royal Road, Springfield, VA 22161

13. SUPPLEMENTARY NOTES

14. ABSTRACT
This investigation focuses on two case histories to develop failure modes under loadings similar to earthquakes. The models are intended primarily to produce cases which can be compared to computer analyses. The first is a $\frac{1}{50}$ scale model of the Koyna Gravity dam section, which cracked during an earthquake. This is a simpler model using a 2-dimensional cross section and no water in the simulation. The second model is a simulation of an arch dam in a wide canyon with a reservoir in flight. Conclusions are stated for trends observed.

15. SUBJECT TERMS

16. SECURITY CLASSIFICATION OF:			**17. LIMITATION OF ABSTRACT**	**18. NUMBER OF PAGES**	**19a. NAME OF RESPONSIBLE PERSON**
a. REPORT	**b. ABSTRACT**	**a. THIS PAGE**			**19b. TELEPHONE NUMBER** *(Include area code)*
UL	UL	UL	SAR		

BUREAU OF RECLAMATION
Technical Service Center, Denver, Colorado
Materials Engineering and Research Laboratory, 86-68180

Report DSO-06-03

Investigation of the Failure Modes of Concrete Dams—Physical Model Tests

Dam Safety Technology Development Program
Denver, Colorado

Prepared: David W. Harris, PhD, PE
Research Civil Engineer, Materials and Engineering Research Laboratory, 86-68180

Checked: Veronica Madera
Civil Engineer, Materials and Engineering Research Laboratory, 86-68180

Technical Approval: William Kepler, PhD, PE
Group manager, Materials and Engineering Research Laboratory, 86-68180

Peer Review: Larry Nuss
Technical Specialist, Structural Analysis Group, 86-68110

3/30/07
Date

REVISIONS					
Date	Description	Prepared	Checked	Technical Approval	Peer Review
3/7/06	Final revisions	x	x	x	x

Mission Statements

The mission of the Department of the Interior is to protect and provide access to our Nation's natural and cultural heritage and honor our trust responsibilities to Indian Tribes and our commitments to island communities.

The mission of the Bureau of Reclamation is to manage, develop, and protect water and related resources in an environmentally and economically sound manner in the interest of the American public.

Acknowledgments

This research was sponsored by the Dam Safety Technology Development Program of the Bureau of Reclamation.

Contents

Page

Acknowledgments iii
Introduction 1
2-Dimensional Koyna Dam Cross Section Test 1
Background 1
Physical Model Test 2
Concrete Mix Design and Material Properties 2
Model Construction and Instrumentation 6
Input Motions 9
Test Results 11
Model 1—Cracked Model 11
Model 2—Monolithic Model 15
Conclusions and Discussion 19
3-Dimensional Arch Dam Simulation 20
Previous Work on Shake Tables 20
Introduction 21
Experiment Setup and Procedure 23
Concrete Mix Design and Material Properties 24
Model Construction and Instrumentation 25
Results and Indications of the Models 27
In-Situ Tests for Modal Shape and Frequency 27
Linear Versus Nonlinear Structural Behavior 27
Effect of Joints on Nonlinear Behavior 29
Effects of a Wide Canyon 30
Water in Joints 39
Conclusions 39
Recommendations 40
References 40

Appendix—*Investigation of the Failure Modes of Concrete Arch Dams Using Physical Model Tests,* by David W. Harris and Fred Travers

Tables

No. Page

1 Estimated concrete properties, the associated scale factors, and the model material target values 2

2 Model concrete mix components 3
3 Properties of model materials 4
4 Averaged values of tested properties from dam core 23
5 Estimated concrete properties, the associated scale factors, and the model material target values 24
6 Model concrete mix components 24
7 Models with associated properties 25
8 Typical frequencies of dams 26

Figures

No. Page

1 Stress-strain graphs. 5
2 Load vs. crack width in ⅓-point beam tension. 5
3 Unload-reload test showing plastic behavior of the low-strength concrete. 6
4 First Koyna model mounted on the shake table. The shrinkage crack and eventual failure plane is sketched in. 7
5 Instrument locations. 8
6 Second Koyna model failure plane. 9
7 First Koyna test—horizontal acceleration at the top of the model. 10
8 The seismic record for upstream/downstream motion during the Koyna event. 10
9 Koyna acceleration response spectrum at 5% damping. 11
10 First Koyna model—base acceleration of 0.5 g. 12
11 First Koyna model—base acceleration of 2.25 g's. 12
12 First Koyna model—base acceleration of 2.5 g's. 13
13 First Koyna model—base acceleration of 2.75 g's. 13
14 First Koyna model—displacement at the top of the model. 14
15 Second Koyna model—frequency sweeps. 15
16 Second Koyna model—horizontal acceleration at the base of the model. 17
17 Second Koyna model—horizontal acceleration at the top of the model. 17
18 Second Koyna model—vertical acceleration at the top of the model. 18
19 Second Koyna model—displacement at the top of the model. 18
20 Final failure of Futatsuno arch dam model. 21
21 ISMES wide arch dam model failure. Homogeneous dam shaken to failure with earthquake simulation. 22
22 ISMES test of narrow canyon dam model. 22
23 Model 2—monolithic model accelerations. 27
24 Horizontal-joint model accelerations. 28
25 Vertical-joint model accelerations. 28
26 17x2-joint model accelerations. 29
27 Initial crack normalized to stiffness. 30
28a Monolithic model 2 initial cracking 31
28b Monolithic model 2 final crack 31

29a Model 10—horizontal joint initial failure, south camera 32
29b Model 10—horizontal joint final failure 32
29c Model 10—horizontal joint north view, initial cracking 33
29d Model 10—horizontal joint north view, final failure 33
30a Model 11—vertical joint south view, final failure 34
30b Model 11—vertical joint south view, initial cracking 34
30c Model 11—vertical joint north view, final failure 35
30d Model 11—north view, initial cracking 35
31a Model 11—vertical joint south view, final failure 36
31b Model 11—vertical joint south view, final failure 36
28a Monolithic model 2 initial cracking. 31
29a Model 10—horizontal joint initial failure, south camera 32
30a Model 11—vertical joint south view, final failure 34
31a Model 11—vertical joint south view, final failure 36
32 Approximate location of all initial cracks in different models. 37
33 Mode shapes for typical dam, measured in the field. 37
34 Final crack pattern and mode shapes. 38
35 Cracks accounting for wide canyon effects. 38

Introduction

One of the most studied cases of a dam subjected to earthquake loading is Koyna Dam in India. This 338-foot (103-meter) high dam suffered cracking during a magnitude 6.5 earthquake in 1967 (Chopra and Chakrabarti, 1971). During this event, the ground acceleration in the stream direction reached 0.49 g with a total duration of strong shaking lasting about 4 seconds. At the time of the event, the reservoir was 37 feet below the crest.

Following the Northridge Earthquake in California on January 17, 1994 and the Kobe Earthquake in Japan 1 year later on January 17, 1995, new consideration has been given to the magnitude of the vertical acceleration of seismic events. Continuing concerns about the performance of concrete dams subjected to severe earthquakes has motivated investigation into ways to analyze and predict this performance using nonlinear numerical analysis techniques (Donlon and Hall, 1991). In some cases, linear dynamic analyses indicate high stresses that can only be further studied with nonlinear models.

2-Dimensional Koyna Dam Cross Section Test

Background

Previous studies of the behavior of concrete dams subjected to seismic accelerations have been conducted on single gravity dam monoliths (Niwa and Clough, 1980; Norman, 1986; Tinawi et al., 1998). Chopra and Chakrabarti (1971) and Donlon and Hall (1991) discussed development of a modeling material that would maintain similitude with the prototype. Donlon and Hall's (1991) work compared to linear elastic analysis results. More recent studies have been completed as centrifuge models (Plizzari, Saouma, and Waggoner, 1995; Renzi, 1994). This more recent work was conducted to provide data for comparison to numerical models.

The purpose of this investigation, conducted at the Bureau of Reclamation's (Reclamation) Materials Engineering and Research Laboratory, was to produce results for comparison to nonlinear computer models. The geometry of the model was scaled from Koyna Dam and follows previous work (Donlon and Hall, 1991; Niwa and Clough, 1980). Because a comparison to numerical models that predict failure was to be made, models were formulated that, to the extent possible,

maintained similitude relationships and yet were simple enough for direct comparison with computer-predicted results. To this end, unlike previous studies (Donlon and Hall, 1991; Niwa and Clough, 1980), similitude with reservoir effects was not attempted. This eliminated the need to model coupling effects. Two models were tested—a model with a natural but preexisting crack, and a continuous model cracked during testing.

Physical Model Test

The scale chosen for this model was a $\frac{1}{50}$ scale. Similitude requirements for models have been summarized in other references (Krawinkler and Moncarz, 1980) and estimated properties of Koyna Dam have also been suggested (Donlon and Hall, 1991; Niwa and Clough, 1980). These properties are summarized in table 1.

Table 1.—Estimated concrete properties, the associated scale factors, and the model material target values

Property	Prototype estimate	Scale factor	Target value
E	4,000,000 lb/in^2 (27,940,000 kN/m^2)	50	80,000 lb/in^2 (558,800 kN/m^2)
f_c	4,000 lb/in^2 (27,940 kN/m^2)	50	80 lb/in^2 (558 kN/m^2)
f_t	400 lb/in^2 (2,794 kN/m^2)	50	8 lb/in^2 (55.9 kN/m^2)
Density	150 lb/ft^3	1	150 lb/ft^3
ε_u^c	0.0025	1	0.0025
ε_u^t	0.00012	1	0.00012

Concrete Mix Design and Material Properties

In this study, a new, low-strength concrete mix was designed. Considerable work has been done in previous studies (Donlon and Hall, 1991; Niwa and Clough, 1980; Donlon, 1989) to produce a similitude-appropriate concrete mix. As has been suggested, curing and the associated shrinkage cracking can be problematic in the use of concrete mixes with highly reduced properties. In addition, the use of any lead product to meet density requirements poses special problems for the handling, storage, and disposal of this hazardous substance. This latter problem, in particular, limits the options for commercial mass production of the material and complicates the disposal of it. When modeling nonlinear failures, additional consideration must be given to ensuring that the correct failure mechanism is reproduced at model scale.

The mix for this study used bentonite pellets as a component to reduce strength. The use of bentonite pellets posed a problem logistically as saturation of the bentonite is required prior to mixing. The mix components and proportions for the initial laboratory-mixed concrete and the commercially mixed model concrete are shown in table 2.

Table 2.—Model concrete mix components

Component	Lab mix, lb/yd^3	Volume in mix, ft^3	Model mix, lb/yd^3	Volume in mix, ft^3
Air		0.14 (½% entrapped air assumed)		0.52 (½% entrapped air assumed)
Water	560	8.99	480	7.68
Cement	160	0.82	168	0.86
Bentonite	40	0.25	42	0.26
Sand	1366	8.4	1454	8.87
No. 4 —⅜" gravel	553	3.36	0	0
⅜" - ¾" gravel	829	5.04	1458	8.81

Note: water/cement = 3.5; bentonite/(bentonite+cement) = 20%

The trial mix was initially made in the laboratory with bentonite saturation accomplished overnight. Based on the apparent success of this mix, both shake table models were made using this design. Due to the volume required for a shake table model (6 yd^3), the actual model mix was supplied commercially. For the commercially supplied concrete, it was assumed that saturation would take place in the mixer drum during transit. Water was adjusted from the original design at the plant to decrease sloshing in transit. On site, a slump of approximately 7.5 inches was used as an indicator of a correct mix. Slump was not a good indicator of strength as indicated by changes in the properties of the concrete. Results from the two mixes are shown in table 3.

Breaks for all compressive cylinder tests failed in a classic shear plane typical of concrete of approximately 65 degrees. Other materials were tested in the lab based on lead/plaster combinations as trial mixes. These materials created failure modes not typical of concrete such as horizontal layer crushing. It is clear that not all parameters matched the similitude requirements simultaneously. Changes in mix water had the largest effect. However, as was stated previously, the primary intent was to produce calibration data for testing of computer models.

Table 3.—Properties of model materials

Property	Lab trial results	Apparent scale (dimensional scale target)	Model mix—Koyna I	Apparent scale (dimensional scale target)	Model mix—Koyna II	Apparent scale (dimensional scale target)
Density, lb/ft^3	133.1	0.9 (1.0)	135	0.9 (1.0)		
E, lb/in^2:						
7-day			42,000	89 (50)		
15-day					157,000	25 (50)
28-day	74,000	54 (50)*	55,000	72 (50)		
Rapid loading:					113,000	
15 days	93,457					
28 days			80000			
35 days						
f_c-						
Static loading:						
7-day	50	80 (50)	89 (50)	45 (50)		
15-day					203	20 (50)
28-day	84	48 (50)	154 (50)	26 (50)		
120-day			290			
Rapid loading:						
7-day	70					
f_t						
Static:						
15 days/split tension					27	15 (50)
15 days/beam tension					60	
21 days/direct tension			14	29 (50)		
21 days/beam tension			32			
28 days/split cylinder	12	33 (50)	20	20 (50)		
28 days/beam tension			49			
Rapid loading:						
15 days/split cylinder					52	8 (50)
28 days/split cylinder	22					
$\varepsilon_u{}^c$	0.004	2 (1)	0.005	2.5 (1)	0.004	2 (1)

*Density corrected by E = scale*density = 50[6]

Laboratory testing was done in support of the tests, with standard tests being run (e.g., typical static compression stress-strain data are shown in fig. 1), and specialized tests were used to help assist in the calculation of parameters that may be required in nonlinear computer material models. Typical fracture (crack width versus load-beam test for a standard ⅓-point bending test) data are shown in figure 2, and unload-reload data demonstrating plasticity of the material are shown in figure 3. These tests were not intended to be an exhaustive set of all tests required for published numerical models, but are believed to be representative of the types of data needed.

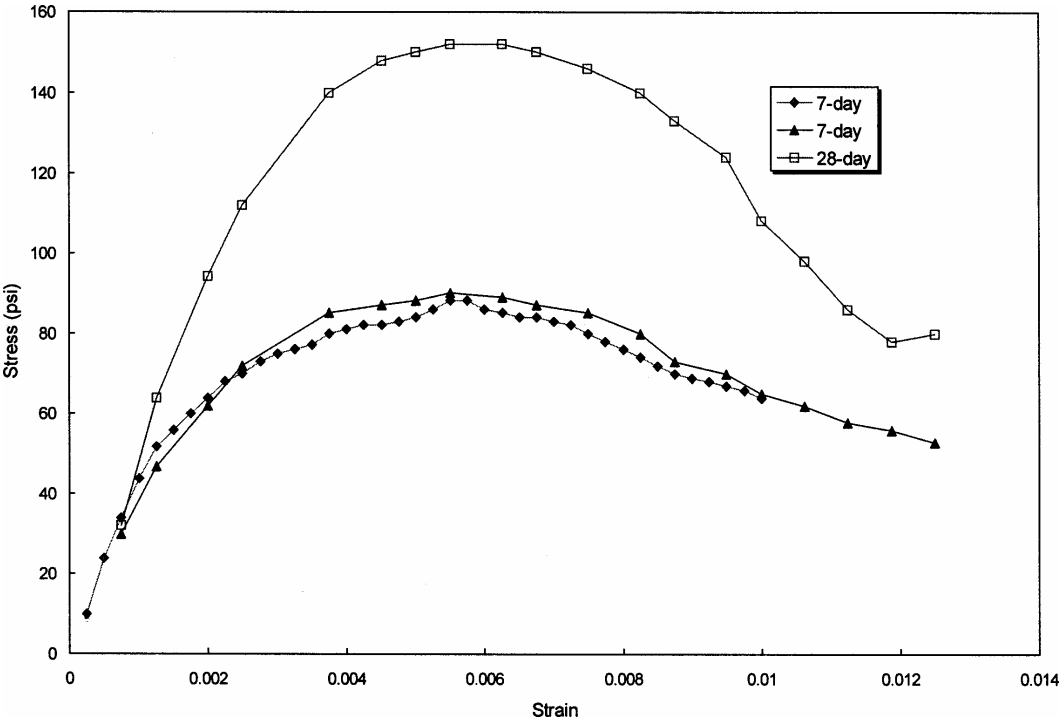

Figure 1.—Stress-strain graphs.

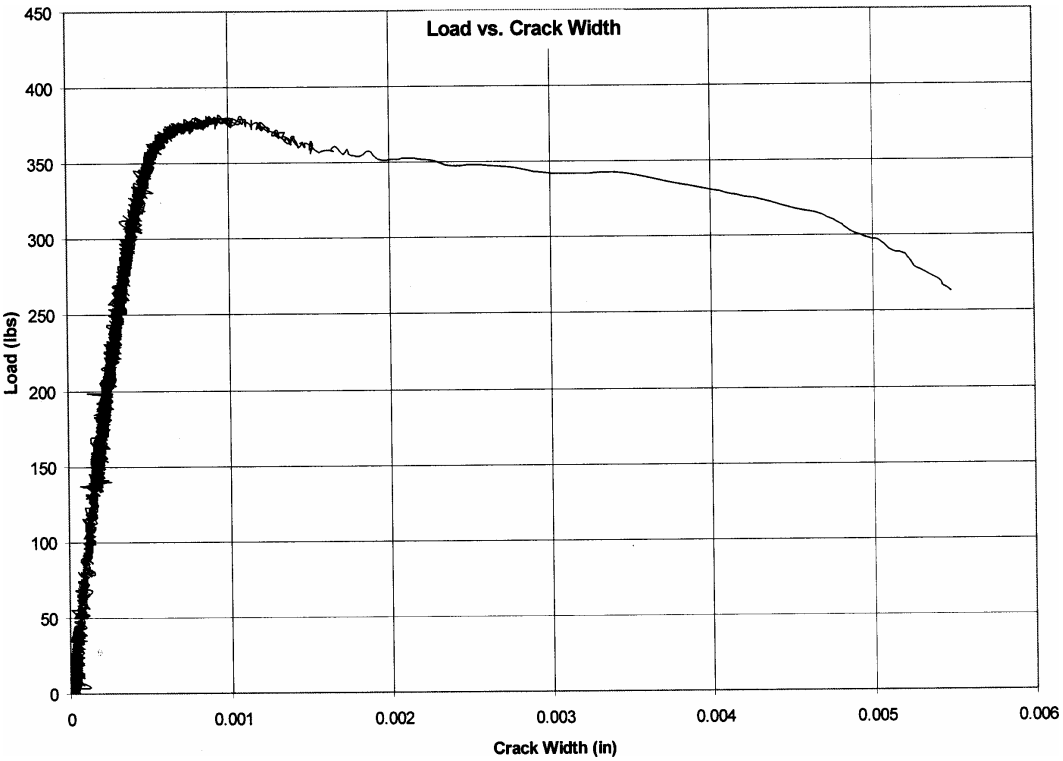

Figure 2.—Load vs. crack width in ⅓-point beam tension.

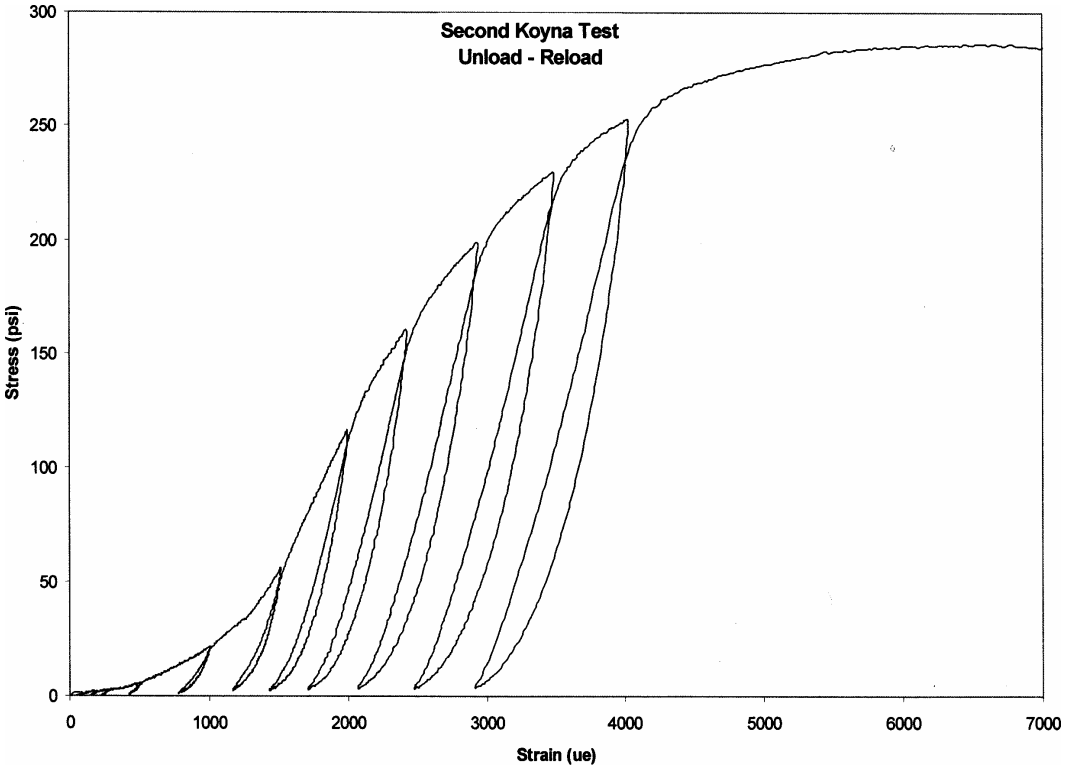

Figure 3.—Unload-reload test showing plastic behavior of the low-strength concrete.

Model Construction and Instrumentation

The tests were performed in Reclamation's Materials Engineering and Research Laboratory. The Vibration Laboratory is used for large scale tests and has been in existence at Reclamation since 1969 (McCafferty, 1970). For these experiments, a shake table was constructed having movement constrained to a single axis (horizontal only). The table was tested for its response modes and also tested in motion with accelerometers to determine its capabilities for use at higher frequencies. The table responded well for input frequencies below 22 Hz, which was below the table-s lowest natural frequency of 30 Hz, but higher frequencies were eliminated for testing. Response of the table was clearly best at frequencies of 26 Hz and below. For this reason, a similitude simulation of an earthquake motion was not used. Rather, for practical reasons associated with the table, and for simplicity in numerical model calibration, a sinusoidal motion was selected.

The model is shown in figure 4 on the shake table. The $\frac{1}{50}$ scale model resulted in an 8.5-foot tall model, figure 5, weighing 7,850 pounds. A slab, representing a foundation, was cast monolithically with the model to provide a fixed lower boundary at the base of the dam. Instrumentation measured displacements and accelerations of the model and input motion of the actuator. The general instrumentation locations are shown in figure 5 and the accompanying table.

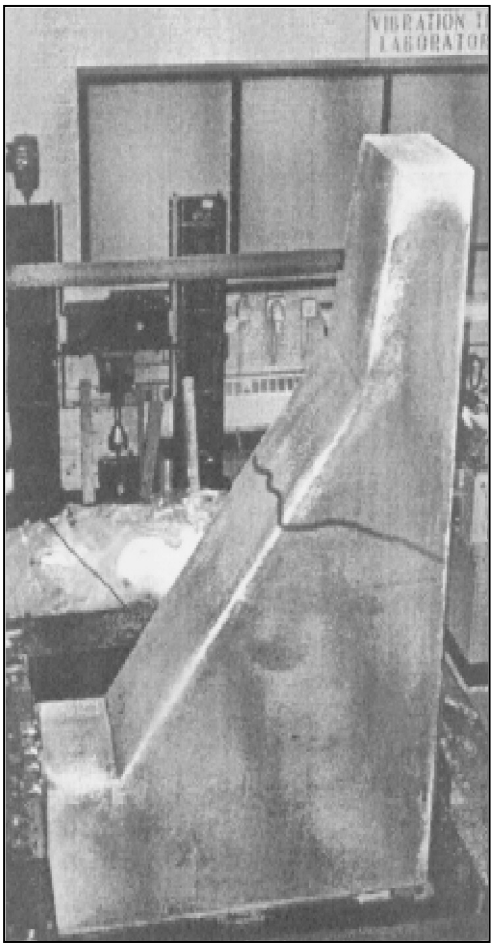

Figure 4.—First Koyna model mounted on the shake table. The shrinkage crack and eventual failure plane is sketched in.

The first model was cast lying down on its side. Form construction and concrete placement were much easier with access to an entire face and only a 1-foot 9-inch depth of material. After approximately 20 days, a small shrinkage crack appeared in the exposed face. At this time, tension tests were run that may be useful in modeling the onset of shrinkage. At approximately 28 days, the model was positioned on the shake table, and the forms were removed. The shrinkage crack was evident on the side of the model, and the sloped face and was assumed to extend through the entire model. The plane of the crack had an inclination of approximately 20 degrees from horizontal toward the side of the model. After approximately 1 additional week, the surface had dried sufficiently to apply instrumentation, and the test was run.

The second model (fig. 6) was cast upright on the shake table to avoid the shrinkage cracking experienced in the first model. By testing earlier, the onset of shrinkage cracking was avoided, and the second model produced a material failure under dynamic loading. Earlier testing also held the model concrete

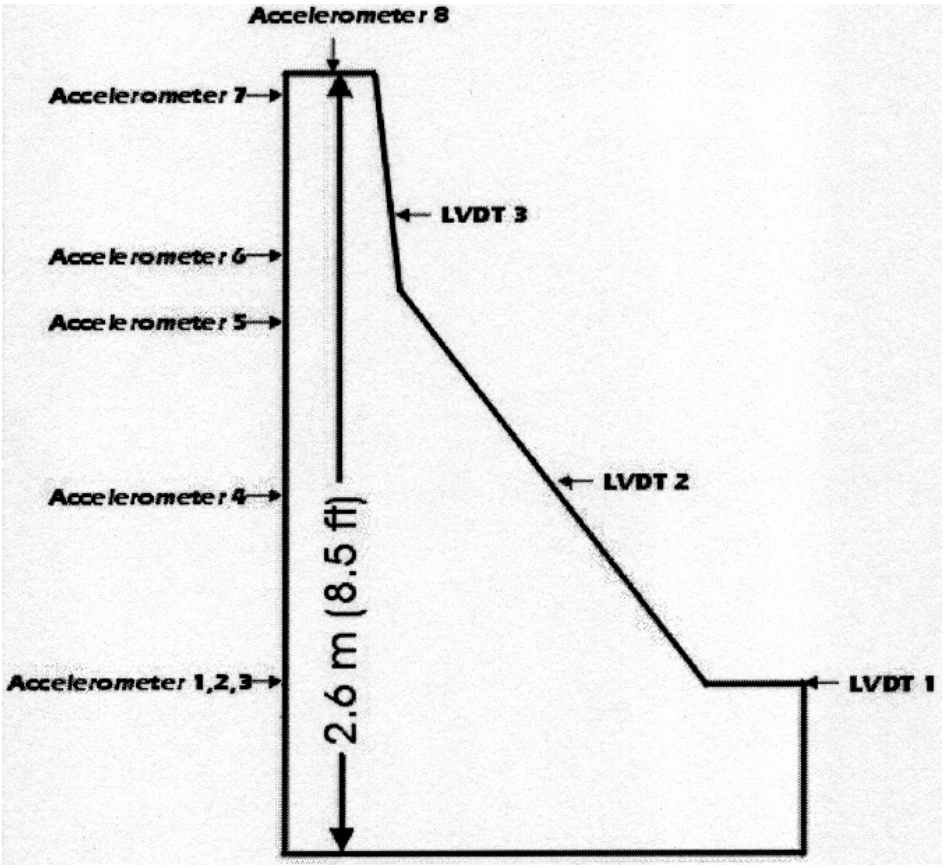

Figure 5.—Instrument locations.

Instrument ID	Type	Orientation	Height from base
Accelerometer 1	Acceleration	Horizontal, x-direction	0
Accelerometer 2	Acceleration	Horizontal, y-direction	0
Accelerometer 3	Acceleration	Vertical, z-direction	0
Accelerometer 4	Acceleration	Horizontal, x-direction	0.66 m (2.17 ft)
Accelerometer 5	Acceleration	Horizontal, x-direction	1.22 m (4.00ft)
Accelerometer 6	Acceleration	Horizontal, x-direction	1.47 m (6.67 ft)
Accelerometer 7	Acceleration	Horizontal, x-direction	2.03 m (6.67 ft)
Accelerometer 8	Acceleration	Vertical	2.6 m (8.5 ft)
LVDT 1	Displacement	Horizontal, x-direction	0
LVDT 2	Displacement	Horizontal, x-direction	0.97 m 3.17 ft)
LVDT 3	Displacement	Horizontal, x-direction	1.69 m (5.54 ft)

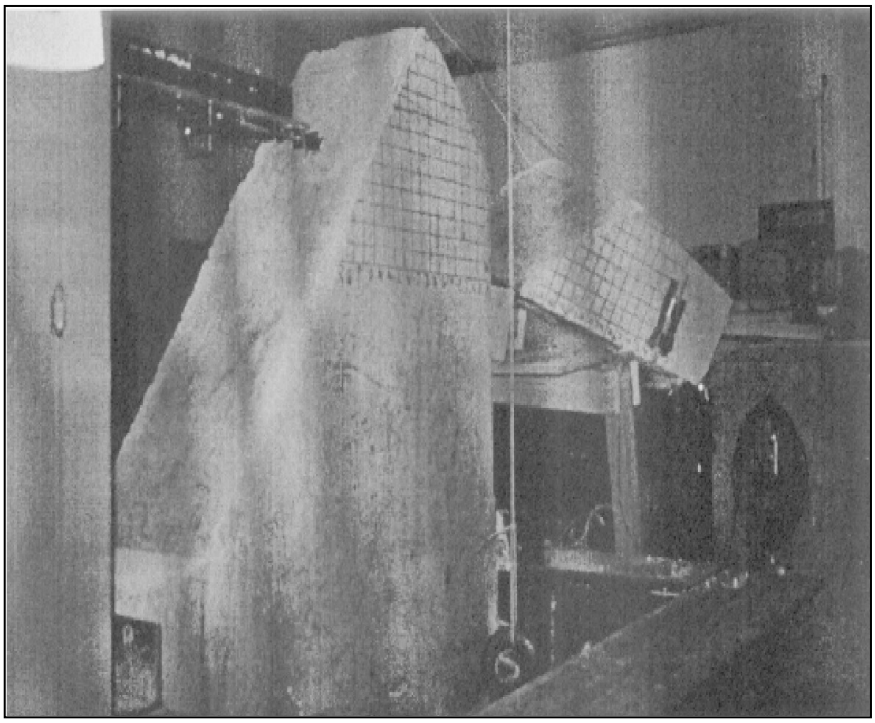

Figure 6.—Second Koyna model failure plane.

strengths lower. Laboratory testing was performed on test specimens of the same material immediately following the breaking of the model.

Input Motions

Numerical analysis predicted that the frequency of the fundamental mode of the model was approximately 14 Hz, but this fundamental mode was out of the plane of the test, that is, side to side in the 2-D model. The cantilever mode, mode 2 of the model but the first mode in plane of the test, was predicted at approximately 28 Hz. Modal sweeps were run on the model at frequencies starting at 2 Hz and increasing to 28 Hz with a constant input acceleration of 0.1 g. The results are shown in figure 7. The first input frequency that showed an increase of acceleration above the input of 0.1 g was 14 Hz. The effect was demonstrated in the plane of testing. Higher frequencies did produce a more dramatic effect. A sinusoidal motion of 14 Hz (approximately 2 Hz prototype) was chosen for the input for all subsequent calibration tests as this lowest response frequency was believed to be the easiest for numerical simulation and calibration. The earthquake record for upstream/downstream motion of the Koyna event (see fig. 8) is believed to have a primary component at 2.4 Hz, a 0.42-second period.. This is more readily seen in the response spectrum of figure 9. With this set frequency of 14 Hz, the accelerations that developed in a single horizontal direction (upstream and downstream to the model) were increased until failure occurred.

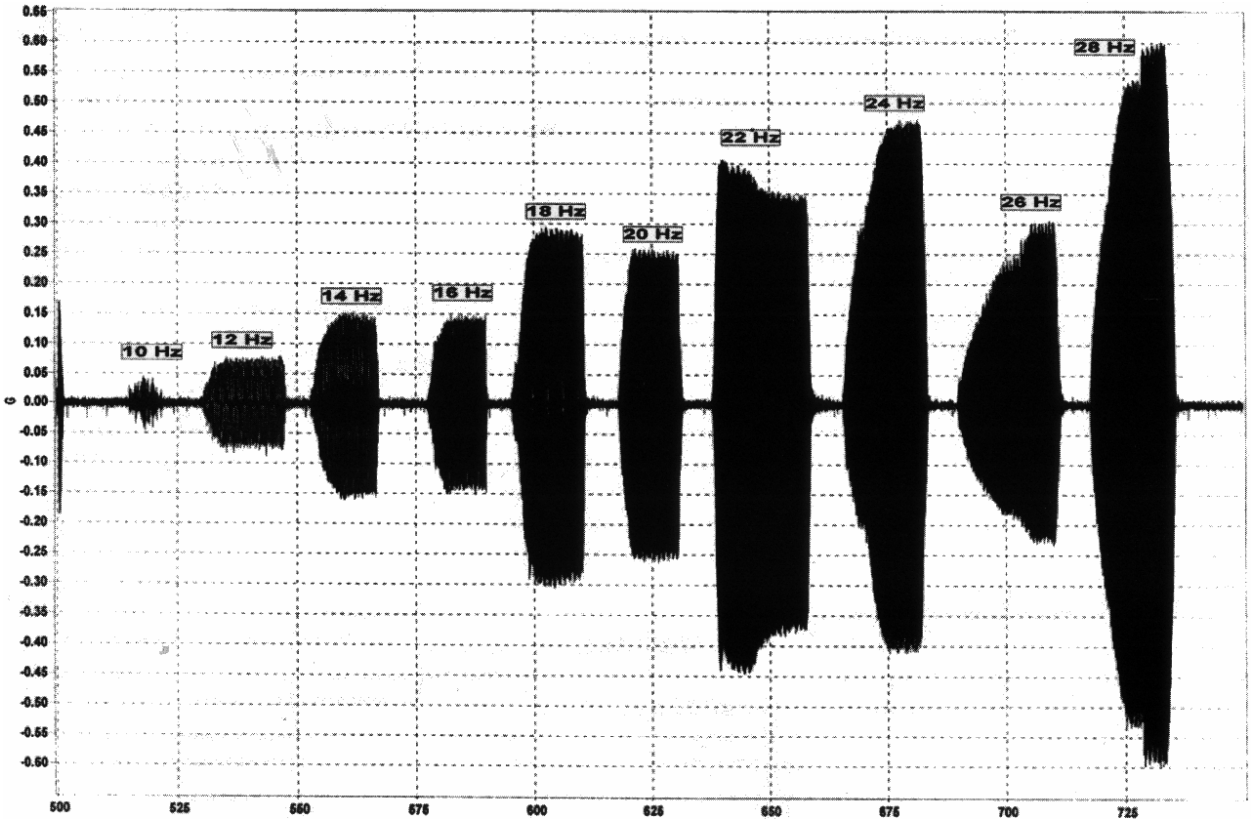

Figure 7.—First Koyna test—horizontal acceleration at the top of the model.

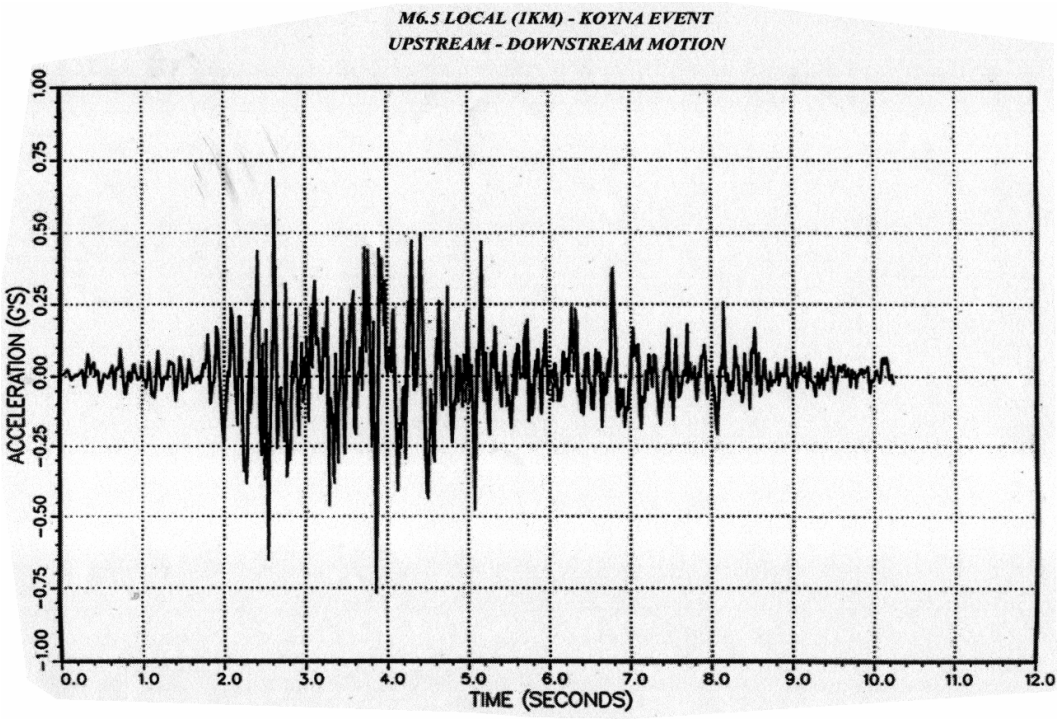

Figure 8.—The seismic record for upstream/downstream motion during the Koyna event.

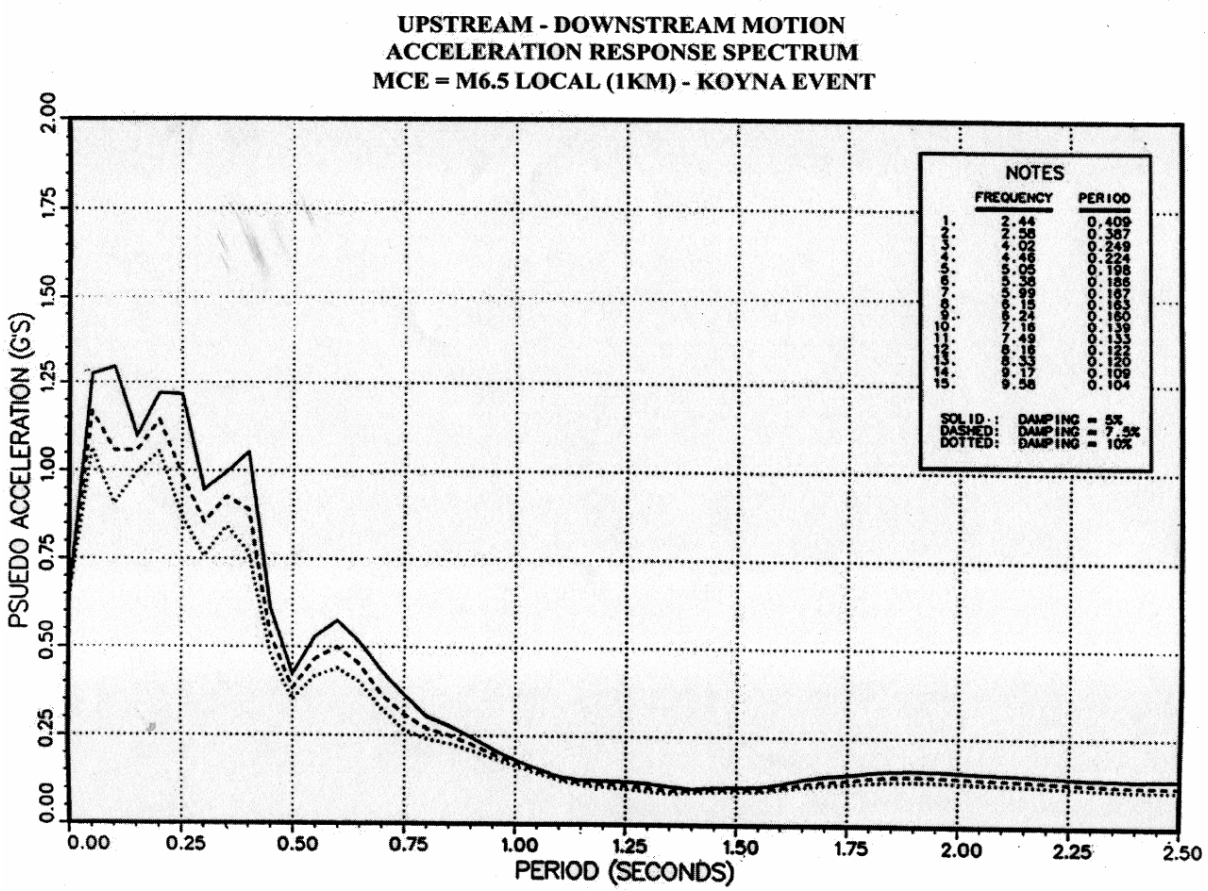

Figure 9.—Koyna acceleration response spectrum at 5% damping.

Test Results

As mentioned above in the discussion of the input motion, the chosen input motion for the model was a 14-Hz sinusoid.

Model 1—Cracked Model

Four typical acceleration plots are shown in figures 10 through 13 for model 1. In figure 10, the acceleration of the base of the dam and the acceleration at the base of the known crack were measured to be 0.5 g, while the acceleration of the crest of the model measured nearly 2 g's. This magnification of acceleration with height from the base of approximately 4 times, is similar to tests reported in the literature (Donlon and Hall, 1991; Niwa and Clough, 1980). The model did not show failure characteristics at this acceleration, which corresponds to the field case.

As this model was to be used with computer programs to model sliding failure mechanisms, testing was continued. Base accelerations were increased while maintaining the 14-Hz input motion. From this point, the constant input frequency has the advantage of seeing changes in response as model

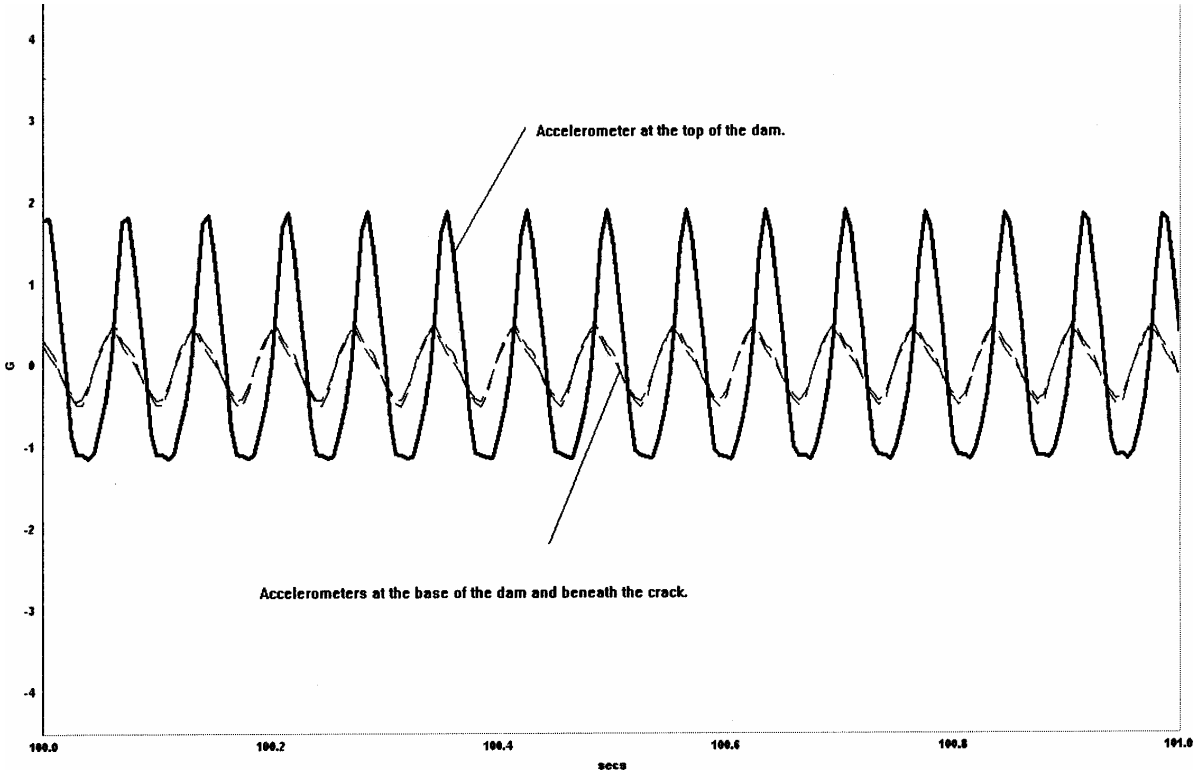

Figure 10.—First Koyna model—base acceleration of 0.5 g.

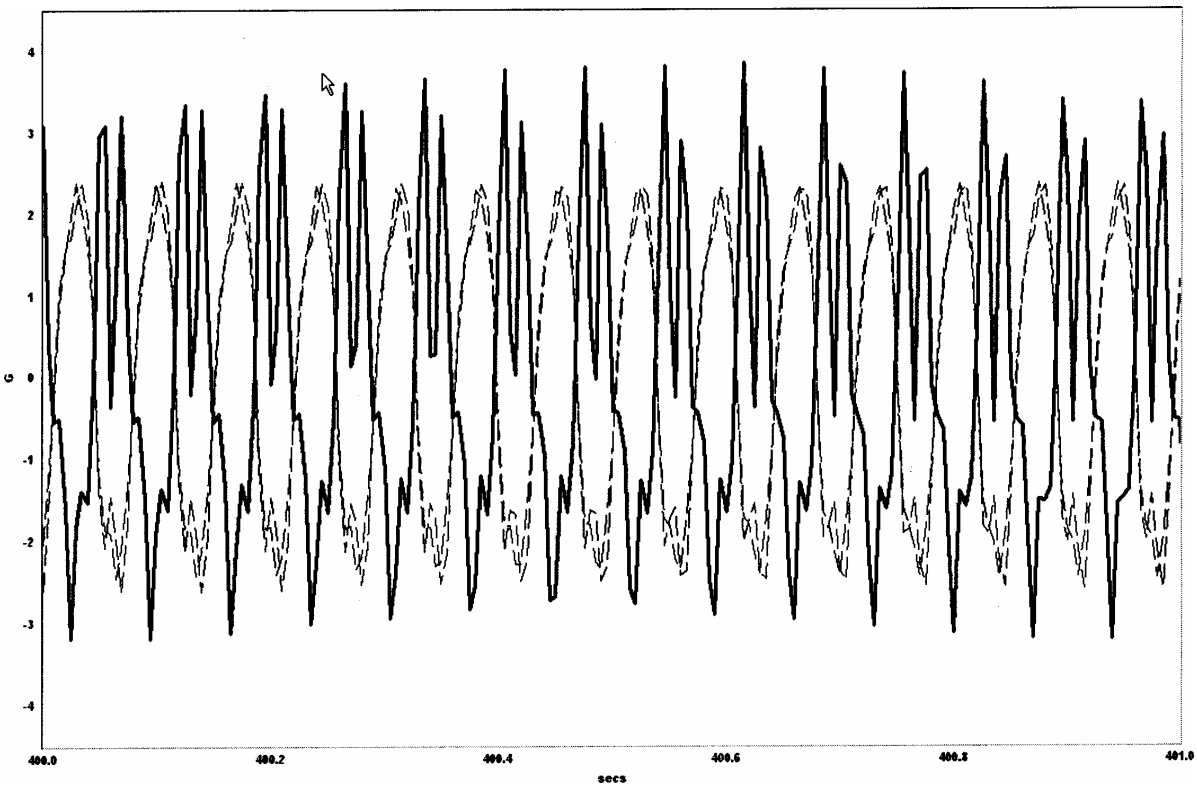

Figure 11.—First Koyna model—base acceleration of 2.25 g's.

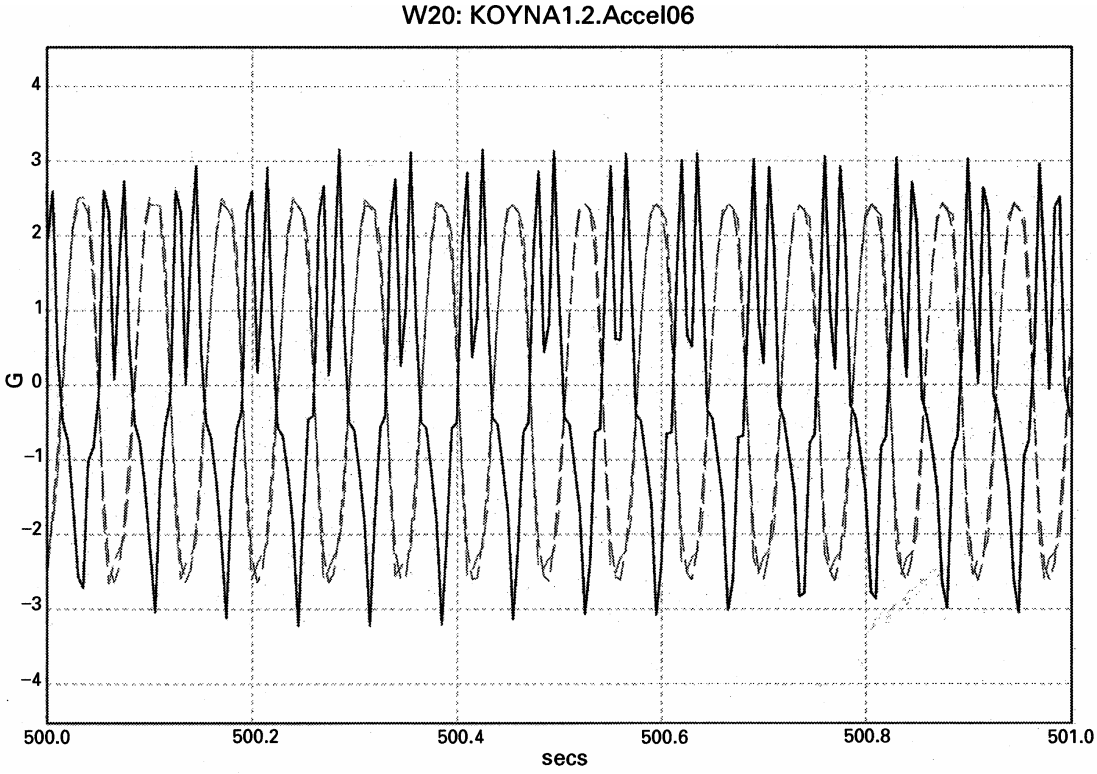

Figure 12.—First Koyna model—base acceleration of 2.5 g's.

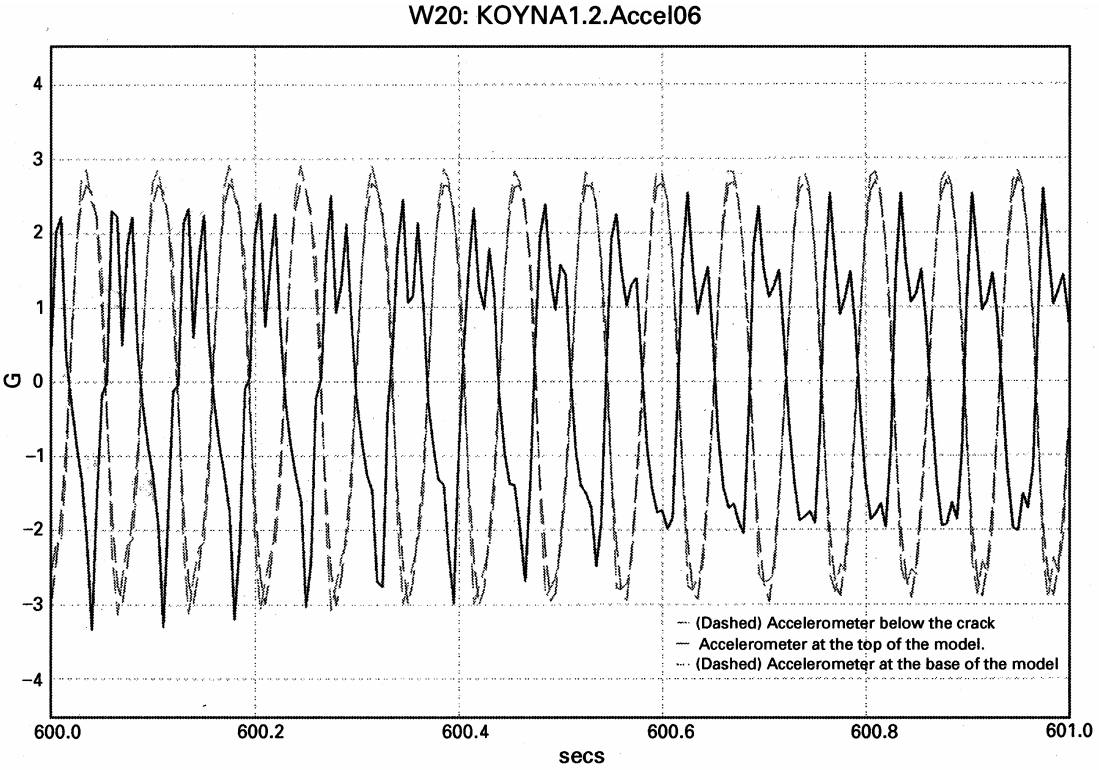

Figure 13.—First Koyna model—base acceleration of 2.75 g's.

characteristics change. At about a 2-g acceleration at the base, a puffing of material from the crack was observed. This was caused by a rocking motion of the top piece of the model (the block above the crack), which acted as a bellows, blowing worn material from the cracked surface.

The next increment in acceleration, at a base acceleration of 2.25 g's showed a change in response of the portion of the dam above the crack. As can be seen in figure 11, the magnification of acceleration from base to top attenuates, showing a maximum of 3.75 g's or a magnification factor of 1.6 times. There is evidence of a phase shift of motion between the top and bottom at this time in the testing.

The next ramp of acceleration was to an acceleration of 2.5 g's of the base. As can be seen in figure 12, with this acceleration, the top and bottom of the model show nearly equal acceleration, with a full 180-degree phase shift between the pieces. As can be seen in figure 14, which shows displacement at the top of the model, the top of the dam is sliding along the base by this time.

Finally, at a base acceleration of 2.75 g's, the bottom motion is at a higher acceleration than the top of the dam (fig. 13). By this time, the displacement of the top piece is well under way, approximately 2 inch (fig. 14), and the base

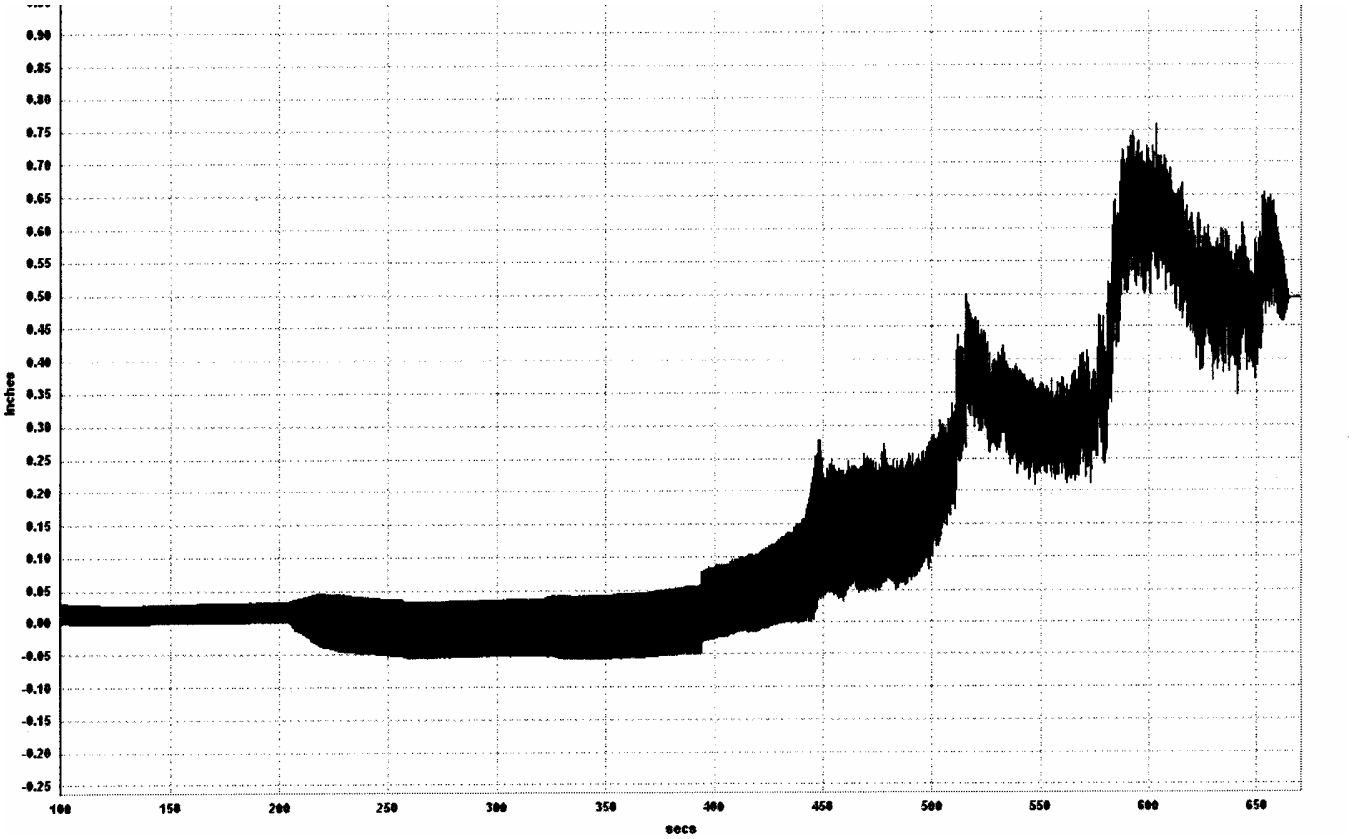

Figure 14.—First Koyna model—displacement at the top of the model.

motion is not readily transferred to the top section. The cross section maintained stability, and sliding progressed slowly during the input. The top block could be observed to be progressively sliding down the preexisting shrinkage crack surface.

Model 2—Monolithic Model

As with the first model, a modal sweep was completed first. Accelerations, normalized to the base motion and recorded during the sweep, are shown in figure 15. In comparing the modal responses with those for the first model, shown in figure 7, some differences are noticed in the response frequencies. In model 1, 24 Hz seemed to indicate the first cantilever mode. In model 2, the first modes that show an amplification factor above the input 0.1 g are 20 Hz and 22 Hz. Review of the directional component shows that this mode appears to emerge at 22 Hz. In both models, another increased response with respect to the input motion occurs at 28 Hz. These differences are believed to be inherent differences in the two models as built, but generally the two models appear similar in their modal response.

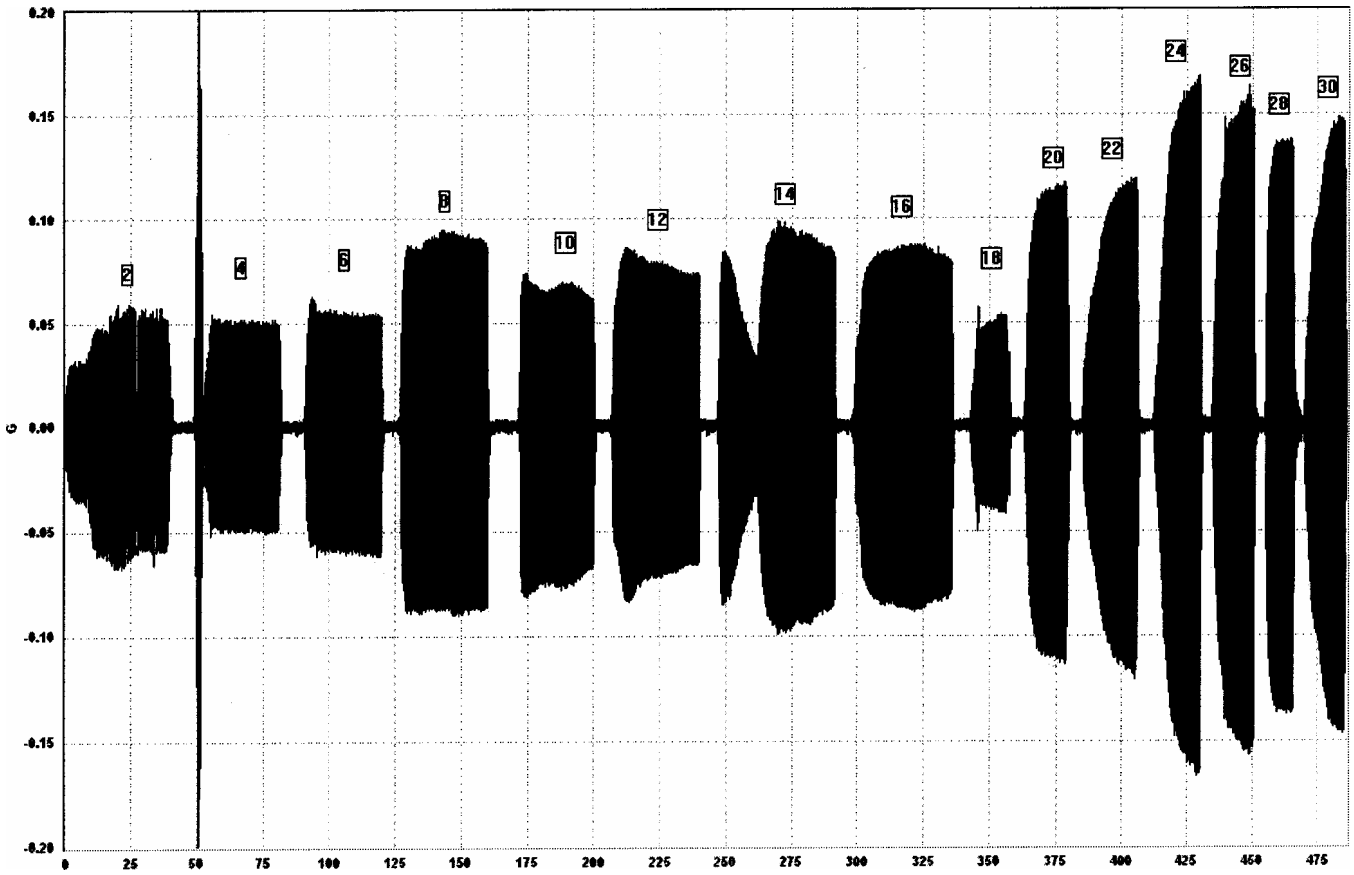

Figure 15.—Second Koyna model—frequency sweeps.

Model 2 was tested using the same strategy as the first model, that is, a 14-Hz sinusoidal motion was used and ramped in acceleration until failure. The total test duration using this method was almost 8 minutes. The final failure occurred at the change in slope of the model on a flat downward plane sloping toward the upstream face. The angle of the failure plane was 53 degrees from horizontal, which was 90 degrees from the lower slope in the bottom of the model, beginning at the invert. This angle is consistent with previous studies (Niwa and Clough, 1980) but was a single flat surface.

The model was videotaped during testing. Review of the tape revealed that the crack was not visible in one frame and had propagated completely by the next video frame. The standard video frame rate is approximately $\frac{1}{30}$ of a second. With the input motion of 14 Hz, the period for 2 cycle would be $\frac{1}{28}$ of a second. This indicates that the crack developed and propagated in less than 0.03 second, either during a stroke, or more probably, at the reversal of a stroke. The base acceleration at the time of failure was 2.2 g's.

Analysis of the test data revealed anomalous behavior beginning approximately 330 seconds into the test (figs. 16-19). This behavior is most prominently displayed in figure 18, which is the vertical acceleration of the model measured at the top of the structure. It can be seen that up to the 330 second point in the test, the vertical acceleration increases linearly with increasing horizontal input acceleration. This response is as expected and is attributed to a slight flexing of the shake table frame. At around 330 seconds, the vertical acceleration starts increasing dramatically and continues to increase throughout the duration of the test. This increase is accompanied by a corresponding decrease in the horizontal acceleration of the top of the structure as seen in figure 17. Figure 19 shows a rather abrupt decrease in the displacement of the top, which would correspond with the decreased acceleration. These phenomena are not believed to be related to the failure of the dam portion of the model, but rather appear to be a failure in the base of the model, which acted as the foundation of the structure.

The conclusion from these data is that the material around the all-thread embedded in the base started failing at around 330 seconds and allowed the model to rock. As more material failed, the rocking increased, which resulted in the increasing vertical accelerations and decreased acceleration of the top, initially. Eventually, the material failure around the all-thread was severe enough that the entire model could slide back and forth a small amount in the direction of the excitation. This is evidenced by the spikes in base acceleration shown starting around 400 seconds in figure 16. This indeterminate boundary condition would be nearly impossible to model on a nonlinear analysis time-step basis. It is believed that general comparisons can still be made based on the final acceleration and the material properties presented.

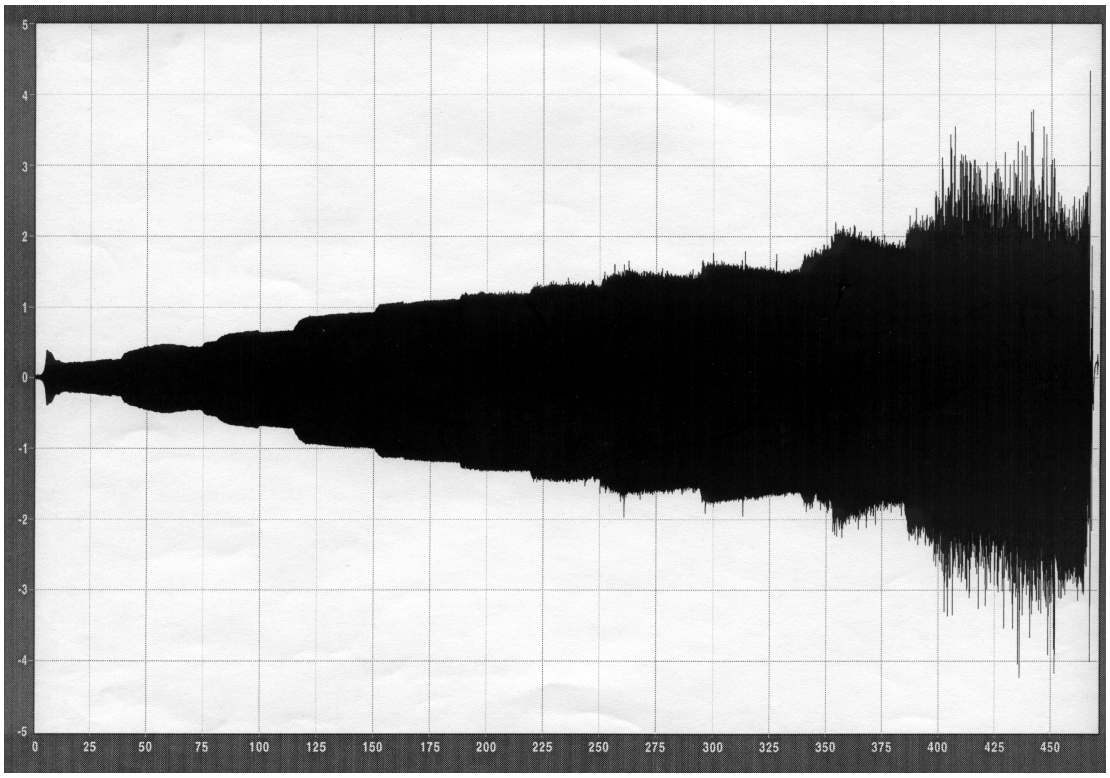

Figure 16.—Second Koyna model—horizontal acceleration at the base of the model.

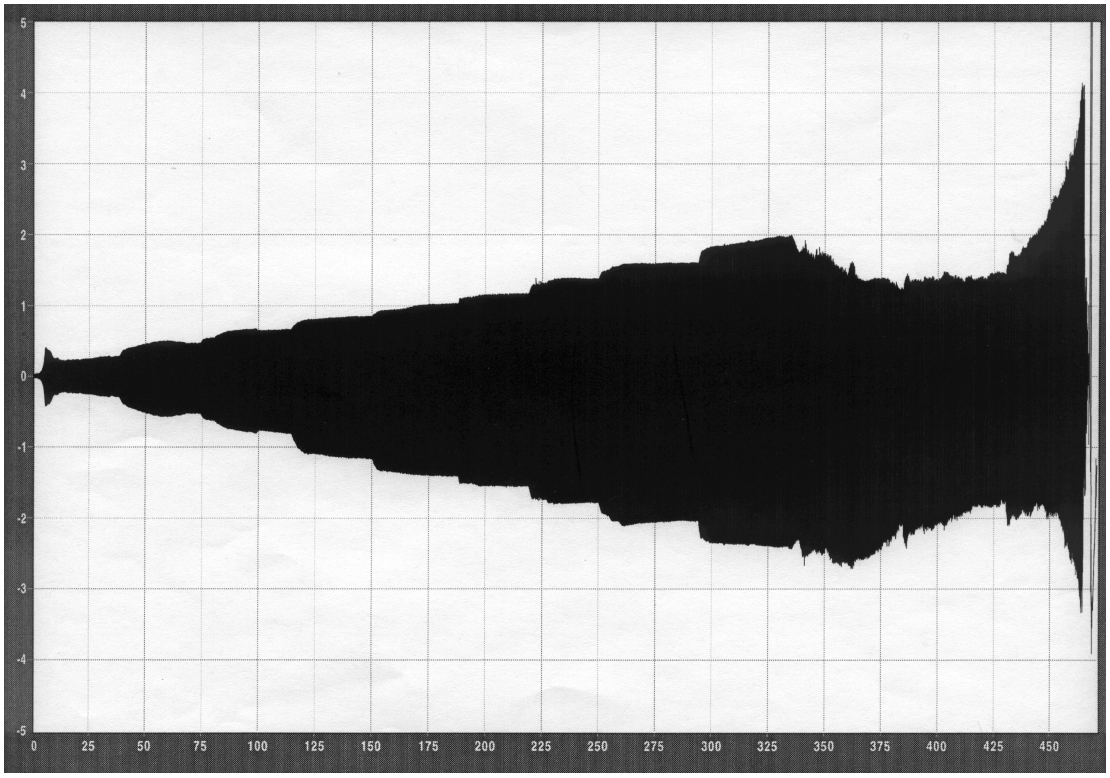

Figure 17.—Second Koyna model—horizontal acceleration at the top of the model.

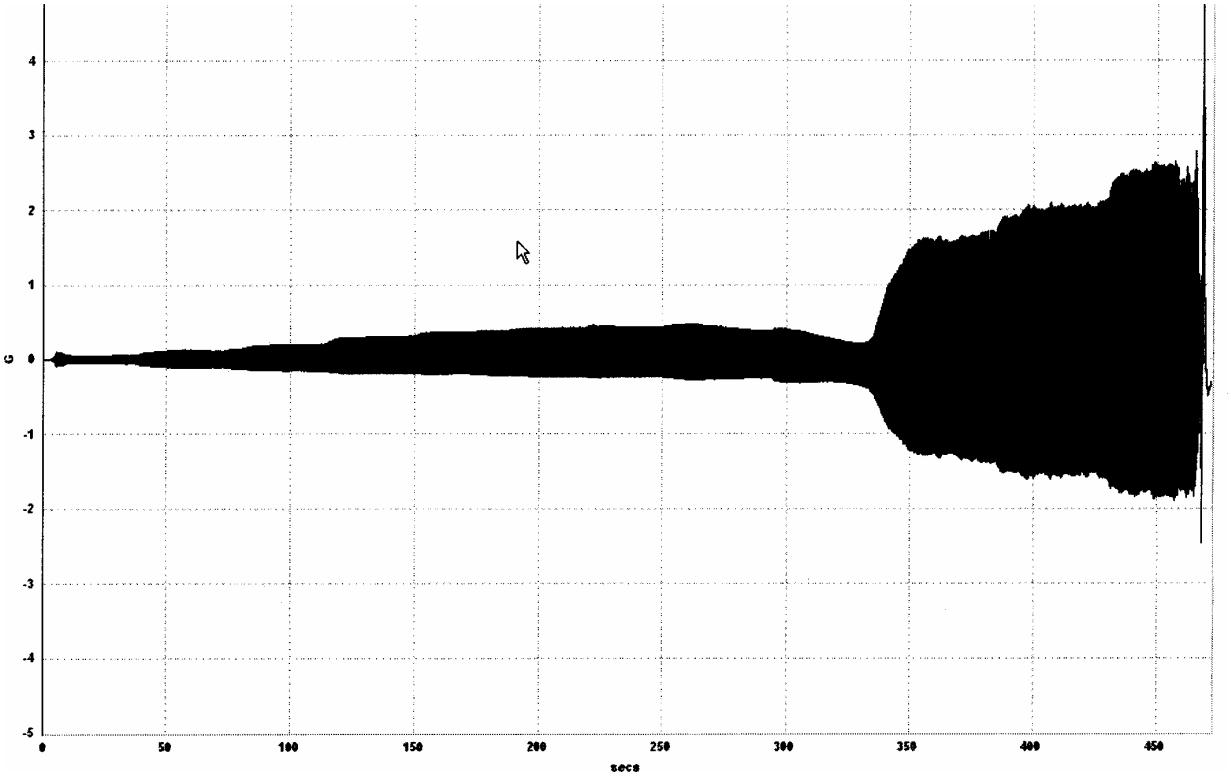

Figure 18.—Second Koyna model—vertical acceleration at the top of the model.

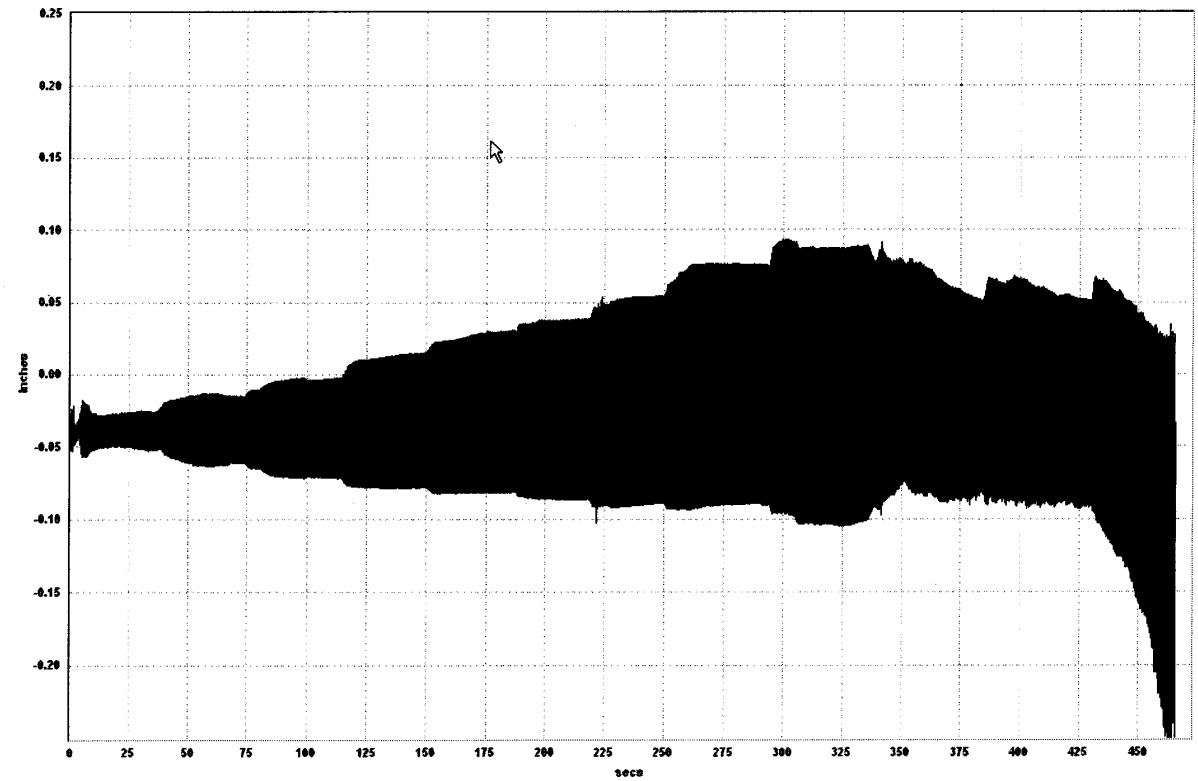

Figure 19.—Second Koyna model—displacement at the top of the model.

It was noted that after initiation of the crack, the top of the model began to slide before toppling occurred. The top portion toppled from the model approximately 1 second (14 cycles) after crack propagation.

Conclusions and Discussion

1. A new low-strength concrete mix is proposed that shows promise for use in similitude testing. The mix, which uses bentonite as the media to reduce strength properties, is readily adjusted to various scales. The components may be mixed en masse and can be provided by commercial producers because no hazardous materials are used. Disposal is also easily accomplished by conventional methods.

2. The new mix produced strength and stiffness characteristics that nearly matched the similitude requirements. More importantly, for nonlinear modeling of the failure mechanism, the mix fails in a shear plane almost identical to that of conventional concrete.

3. The initially cracked model and the monolithic model showed general mode shapes and damping that were similar for small accelerations.

4. The kinematically nonlinear model (sliding model) demonstrated that there was some initial bond on a typical shrinkage crack, even a crack visible to the eye on multiple faces, which needs to be overcome before sliding can be initiated.

5. Once sliding starts, the nonlinear effect creates very large changes in the dynamic response under a constant frequency sinusoidal input motion. The amplitude of the acceleration of the piece above the crack in this model actually becomes less than the amplitude of the acceleration of the base, and the response is phase shifted. Put simply, the base can slide back and forth beneath the top with the motion being nearly uncoupled.

6. The monolithic model failed with a material failure that was characteristic of previous models and believed to be characteristic of cracks in the field.

7. During the monolithic test, a nonlinear change in the base fixed-boundary condition created a highly nonlinear and indeterminate boundary condition. This nonlinear change also showed large changes in the dynamic response of the model, which are easily seen when compared to the constant input motion. Unfortunately, this same boundary condition change makes exact time history matching of numerical models impossible.

8. Both models failed at approximately 2.2 g's of acceleration. In the kinematic model, the crack allowed a slow progressive sliding during the cyclic motion. In the materially nonlinear model, a crack was initiated in less than $\frac{1}{30}$ of a second and sliding occurred for a number of cycles before the top of the

model toppled. The toppling is inconsistent with previous models and is believed to be related to the vertical accelerations caused by the boundary condition change.

9. Laboratory tests of the material were performed in conjunction with the shake table models to provide parameters typically needed in nonlinear numerical material models.

10. Results from the kinematic failure model (sliding) can conceivably be time step matched to verify nonlinear models. Results from the materially nonlinear models can be verified in a general manner to verify the cracking pattern and acceleration required for failure.

3-Dimensional Arch Dam Simulation

Previous Work on Shake Tables

The arch section of the Techi Dam, Taiwan, has been modeled at a scale of $1/150$ (Niwa and Clough, 1980). A primary purpose of that study was to model the opening of joints; thus the dam was articulated. The model was tested with motion in two planes, upstream/ downstream and cross-canyon. Vibration mode frequencies were tested by suspending a weight from the model and subsequently cutting the weight loose to produce face vibrations. The El Centro Earthquake record was used in the shake table model test with a time reduction of $\sqrt{1/150}$. Intensity was increased until the model collapsed. Significant joint degradation occurred at the arch end, probably due to local crushing at one end. In biaxial excitation the arch collapsed with 1.34-g acceleration in the upstream/downstream direction and 0.91 g in the cross-canyon direction. The collapse occurred surprisingly close to the end of the excitation.

The same authors (Niwa and Clough, 1982) noted that the test results showed significant nonlinear behavior. Significant influence of the joints generated increasingly poor correlations with the numerical analysis. Crushing in joints is suggested to improve analytical results.

Other tests have been conducted with shake table models (Oberti, and Castoldi, 1981) on smaller scale models at a scale of $1/100$ and were tested to failure. A sinusoid input motion was used to determine characteristic frequencies of the structure. Next, similitude-corrected time histories of seismic events were used at increasing amplitudes to induce failure. Natural frequencies appear to be produced correctly when the foundation is carried 1 to 2 times the height of the dam both depthwise and in the lateral directions. The length of the reservoir

shows no significant effect in the failure modes with reservoir length being 2 times the dam height.

Test models have been completed to model sliding only (Mir and Taylor, 1996). Typically, these models were 1,000 mm in height. A short reservoir tank with absorbent rubber was used to eliminate the hydrodynamic effect (the tank was 0.4 m in length). The input motions used were (1) a 7.5-Hz sine wave (this waveform was hard to match exactly because some free vibration was present in table), (2) 5 Hz ramped up in 5 cycles, held for 10 cycles, then ramped down in 5 cycles, and (3) a simulated earthquake of 12 seconds duration with the input ramped until slipping occurred.

Several models have been constructed to simulate failures in dams. One such model was the Futatsuno Arch Dam (Yoshida and Baba, 1965). This 76-meter high, 210-meter crest dam was modeled at $\frac{1}{50}$ scale. In this model, the first crack appeared at 0.27 g and 32 Hz in a spillway pier, and on the dam at 0.41 g and 30 Hz. Final collapse occurred at 0.69 g, and 17 Hz. The final failures are shown in figure 20.

Testing of models run to failure has been conducted at the ISMES facility in Italy with the results shown in figures 21 and 22 for wide and narrow canyons, respectively (Oberti and Castoldi, 1980; Oberti and Lauletta, 1967).

Introduction

All of the models chosen for this study were based on a similar geometry. Models were run in a sequence of (1) a monolithic dam, (2) 1 horizontal joint at approximately mid-height, (3) 1 vertical joint at the mid-point of the valley, and

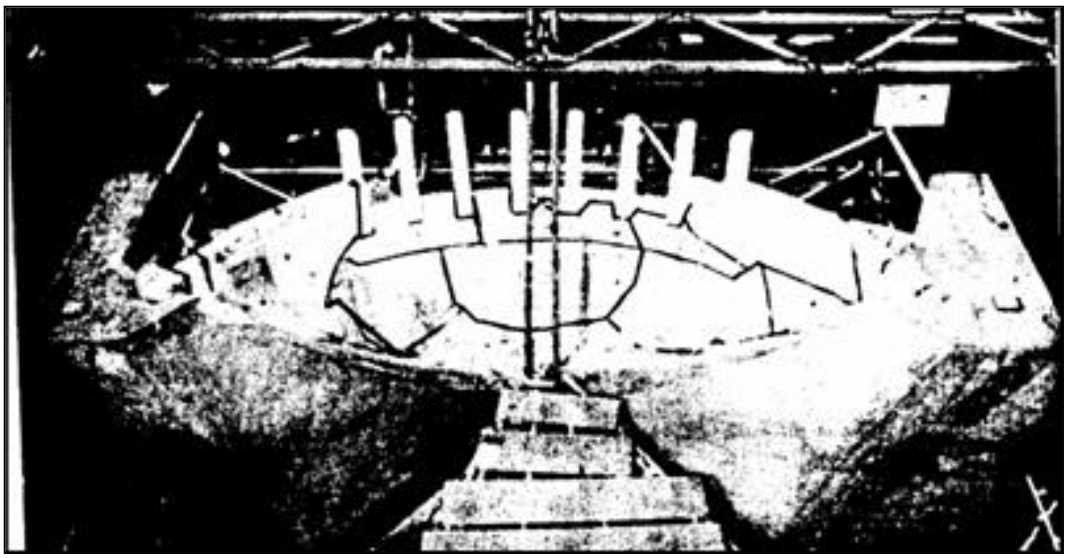

Figure 20.—Final failure of Futatsuno arch dam model.

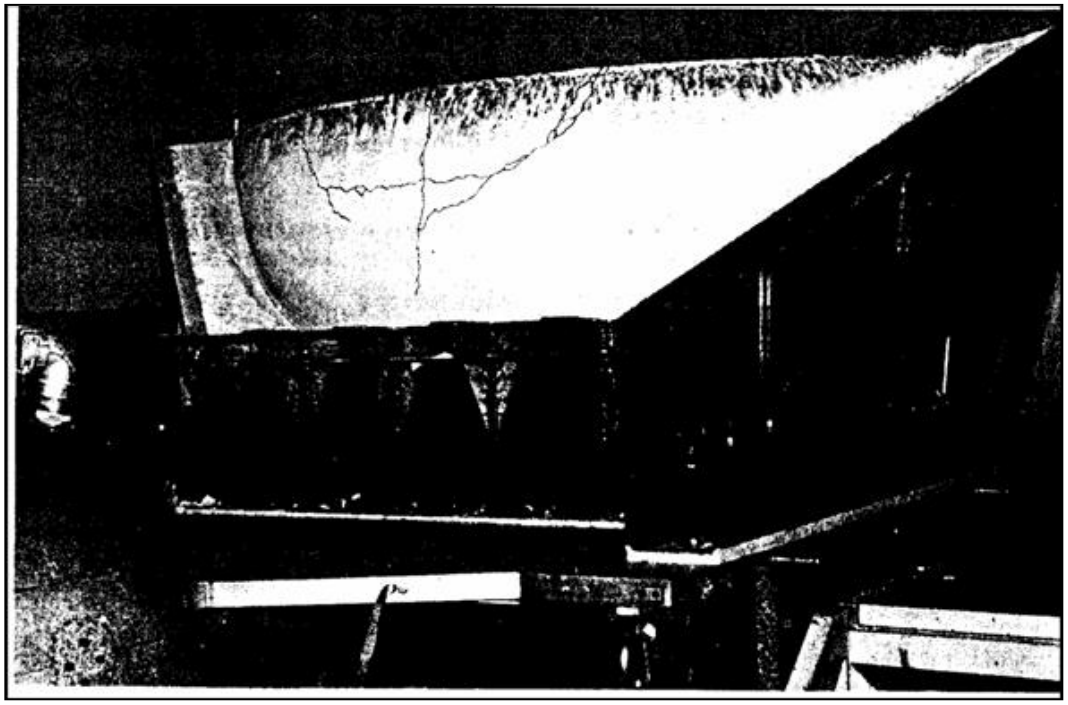

Figure 21.—ISMES wide arch dam model failure. Homogeneous dam shaken to failure with earthquake simulation.

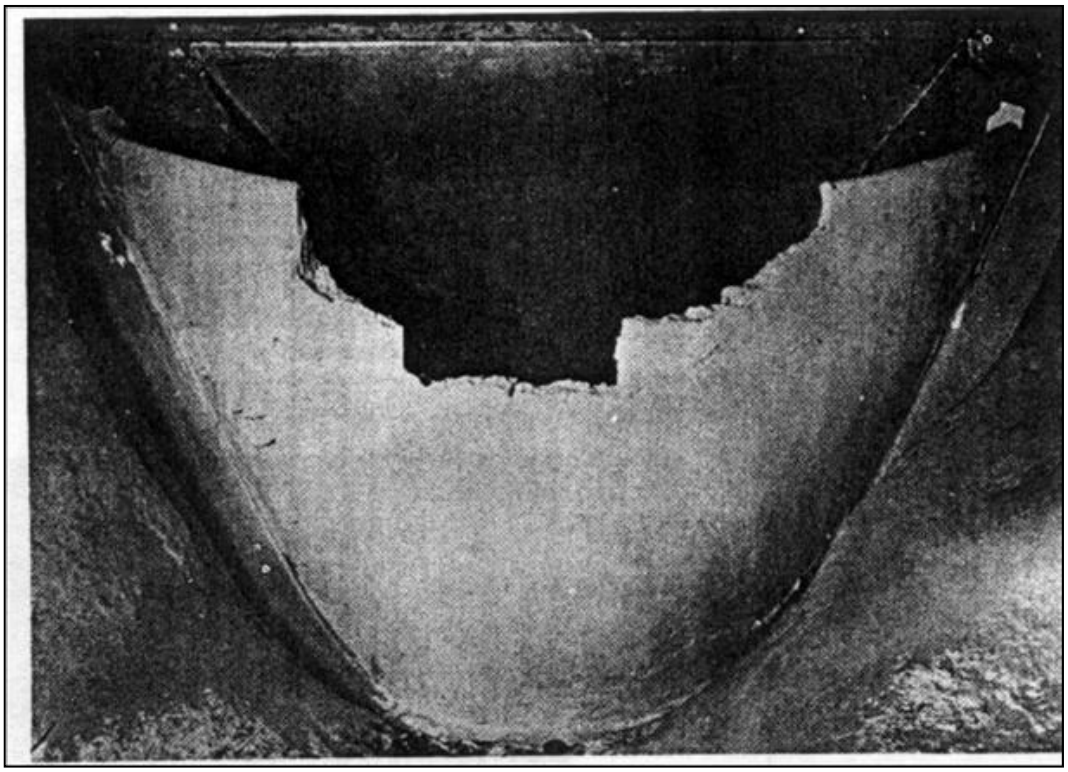

Figure 22.—ISMES test of narrow canyon dam model.

(4) 17 vertical joints and 2 horizontal joints (one model was run with 17 vertical joints as a test of construction method). All models were run with a sinusoidal input motion at 14 Hz beginning at 0.25 g and increasing every 30 seconds by 0.25 g until a structural collapse was created in the model.

Experiment Setup and Procedure

The scale chosen for this model was $1/150$. Similitude requirements for models have been summarized in other references (Krawinkler and Moncarz, 1980). Properties of mass concrete in dams have previously been published (Harris, Mohorovic, and Dolen, 2000) and are summarized in table 4. For this study, typical values of properties were chosen as target parameters for the model and are summarized in table 5. A summary of this work is contained in the appendix and in this presentation it is suggested that the model values fall in appropriate ranges compared to field values.

Table 4.—Averaged values of tested properties from dam core

Dam	Dynamic compressive strength, lb/in^2	Dynamic modulus of elasticity, Mlb/in^2	Dynamic tensile strength, lb/in^2
Pine Flat	5280	3.43	Unknown
Deadwood	5930	3.83	690
Stewart Mountain	5350	3.99	515
Roosevelt Saturated 1a	4090	4.21	755
Roosevelt Air dried 1b	4600	4.09	485
Roosevelt Saturated all other	6430	4.84	840
Roosevelt Air dried all other	4850	4.10	840
Roosevelt 12" diameter Air cured	3730	5.70	575
Hoover	8040	4.33	975
Folsom	4760	4.50	510
Monticello	4870	6.12	505
Englebright	6660	4.63	585

Table 5.—Estimated concrete properties, the associated scale factors, and the model material target values

Property	Prototype estimate	Scale factor	Target value
E	5,200,000 lb/in^2 36,322,000 kN/m^2	150	35,000 lb/in^2 244,475 kN/m^2
f_c-	4,500 lb/in^2 31,432 kN/m^2	150	30 lb/in^2 209 kN/m^2
f_t	450 lb/in^2 3,143 kN/m^2	150	3 lb/in^2 21 kN/m^2
Density	150 lb/ft^3 2,403 kg/m^3	1	150 lb/ft^3 2,403 kg/m^3
$\varepsilon_u{}^c$	0.001	1	0.001
$\varepsilon_u{}^t$	0.0001	1	0.0001

Concrete Mix Design and Material Properties

In this study, a new low-strength concrete mix was designed. Considerable work in this area has been accomplished in previous studies to produce a similitude-appropriate concrete mix (Donlon and Hall, 1991; Niwa and Clough, 1980; Donlon, 1989). Work from Harris, et al. (2000) was used previously with 2-dimensional model studies in Reclamation's Engineering Materials and Research Laboratory. The advantages of this design were discussed previously. This design was modified for the $1/150$ scale models of this study; the mix components and proportions are shown in table 6.

Table 6.—Model concrete mix components

Component	Lab mix, lb/yd^3	Volume in mix
Air		0.14 (½% entrapped air assumed)
Water	739.8	11.86
Cement	156.6	0.8
Bentonite	63	0.39
Sand	2245.41	13.81

Note: water/cement = 4.72; bentonite/(bentonite+cement) = 28.7%

Early tests with this material demonstrated that all scaled parameters desired could not be met simultaneously. Specifically, the modulus of the material was on the order of 3,500 lb/in^2, and density was 118 lb/ft^3. With these constants,

coefficients for calculating the required similitude relations were derived following the modeling theory developed by Houqun et al. (1994). The coefficients used were: $C_E = 4{,}500{,}000/3{,}500$; $C_\rho = 150/118$; and $C_s = 150$, where C_E represents the coefficient for modulus, C_ρ represents the coefficient for density, and C_s is the scale factor. Table 7 introduces the strength and stiffness and the series of models produced for this study.

Table 7.—Models with associated properties

Model	Type	Date	Age, days	Avg. comp, lb/in^2	Avg. split, lb/in^2	Avg. beam, lb/in^2	E	Failure acceleration, g	
								Initial crack	Final failure
M-1	Monolith	3/12/99	7	28.1		3.2			
M-2	Monolith	3/31/99	7	23.25		4	2302.6	0.75	5.0
M-4	Monolith—1st pulse	7/28/99	6	33.64			3761		
M-5	Monolith	8/12/99	6	37.5	4.83	3.1	3088.4		
M-6	Vertical joint (saloon door)	8/27/99	7	25.6	4.67			0.7	0.85
M-7	Vertical joint	5/2/00	8	40.3				1.5	1.5
M-8	Vertical joint	6/21/00	7	28.2				1.5	1.5
M-9	Horizontal joint	7/19/00	7	36				0.95	1.75
M-10	Horizontal joint	8/2/00	7	52.1			5172.1	1.65	1.65
M-11	Vertical joint	8/22/00	6	41.97	4.4		3758.8	1.2	1.2
M-12	17 vertical joints	10/3/00	5	27.01			2146.6	0.6	0.6
M-13	17 vertical joints	4/10/01	5	23.2	3.58		3461.5	0.5	0.5
M-14	2 horizontal, 17 vertical joints	4/24/01	5	19.625	3.09		3099	1	1.25
M-15	2 horizontal, 17 vertical joints	5/1/01	5	21.4	4.05		3948	0.75	0.75

Model Construction and Instrumentation

As discussed in the previous section, sinusoidal loadings were used as input.

The selection of the frequency of the motion was based on the similitude coefficients and typical values of natural frequencies of dams tested onsite. The frequency conversion similitude coefficient becomes:

$$C_f = C_S \frac{\sqrt{C_\rho}}{\sqrt{C_E}}$$

For this model, the scale (C_s) is $1/150$. Considering the range of modulus values of the materials in various models (C_E), a range of frequency coefficients would be from 4 to 5.36. Table 8 shows typical measured values of natural frequencies for specific dams. A typical first mode natural frequency of 3.3 Hz was chosen for a wide valley structure. Applying the range of similitude coefficients to this frequency yields a range of model scale frequencies from 12 to 16 Hz and hence the chosen excitation frequency of 14 Hz. In the summary discussion in the appendix, a discussion of appropriate values is based on ranges of values from field cases.

Table 8.—Typical frequencies of dams (Takahashi, 1964; Rouse and Bouwkamp, 1967; Duron and Hall, 1988; Oberti and Castoldi, 1981; Houqun et al., 1994)

Dam	Reservoir level	Frequency (Hz)					Damping (%)				
		Sym.			Asym.		Sym.			Asym.	
		1st	2nd	3rd	1st	2nd	1st	2nd	3rd	1st	2nd
Kamishiba	Full	3.8	5.8	8.7	4.3	7.2	5	4	4.5	4	4.5
	Low	-	6.3	9.7	4.7	8.0	-	4	4.5	4	4
Sazananigawa	Full	5.5	6.8	-	4.3	8.7	2	3.7	-	3	2
	Low	6.7	-	-	5.5	-	1.8	-	-	1.8	-
Monticello	-	3.13	4.68	7.60	3.55	6.00	2.7	2.5	2.4	2.2	2.1
Morrow Point	-	2.95	3.95	5.40	3.30	6.21	4.0	3.9	4.3	1.5	3.3
Alpe Gera gravity	78%	3.25	-	-	4.56	-	5.4	-	-	5.12	-
	Empty	3.47	6.16	-	4.72	7.43	4.4	4.50	-	4.50	3.43
Fiastra gravity	88%	4.72	7.87	-	5.97	9.72	3.27	2.38	-	2.46	2.50
	72%	4.29	7.34	-	2.56	9.16	3.30	2.80	-	7.34	2.50
Place Moulin arch	95%	2.03	3.63	-	2.03	2.96	1.15	1.20	-	1.18	1.22
Talvacchi arch	90%	3.8	5.35	-	3.68	6.7	3.5	3.5	-	3.5	3.5
Barcis arch	Full	10.1	15.3	-	7.6	16.3	4	4	-	7.0	3.5
Ambiesta arch	Full	4.27	7.3	-	3.90	-	3.02	6.65	-	2.15	-
	94%	4.7	-	-	2.0	-	1.9	-	-	4.7	-

Results and Indications of the Models

In-Situ Tests for Modal Shape and Frequency

Tests were conducted on the model using frequency sweeps at very low accelerations, 0.5 g, to physically test for the model modes. The low acceleration was chosen to ensure that damage would not occur during the frequency sweeps. Unfortunately, the low excitations did not produce sufficient displacement for a conclusive determination of the model's dynamic behavior.

Linear Versus Nonlinear Structural Behavior

The models all acted in a structurally linear manner until the onset of any cracking. This was evidenced by a characteristic mode shape and increase of acceleration from the base of the dam to the top of the dam. This pattern is shown for the monolith, horizontal-only joint, vertical-only joint, and 17x2-joint models in figures 23 through 26, respectively. These figures all show time plots of acceleration over a fairly broad time. From the plots, the increase between top acceleration versus the base of the dam is shown in the overlay of data. The initiation of cracking causes a nonlinear effect, which results in a change in the pattern. A good example of this is shown in figure 24 with an obvious change in response. In figure 25, another model is shown with an expanded scale time.

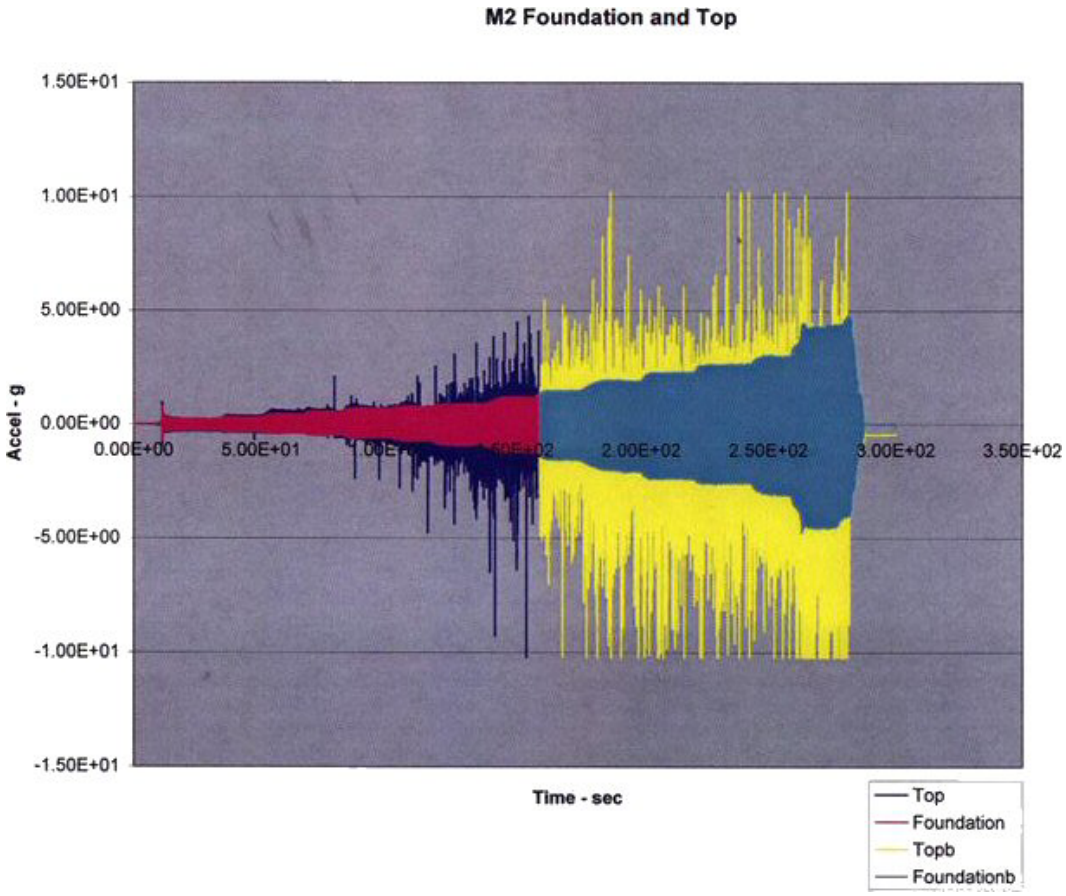

Figure 23.—Model 2—monolithic model accelerations.

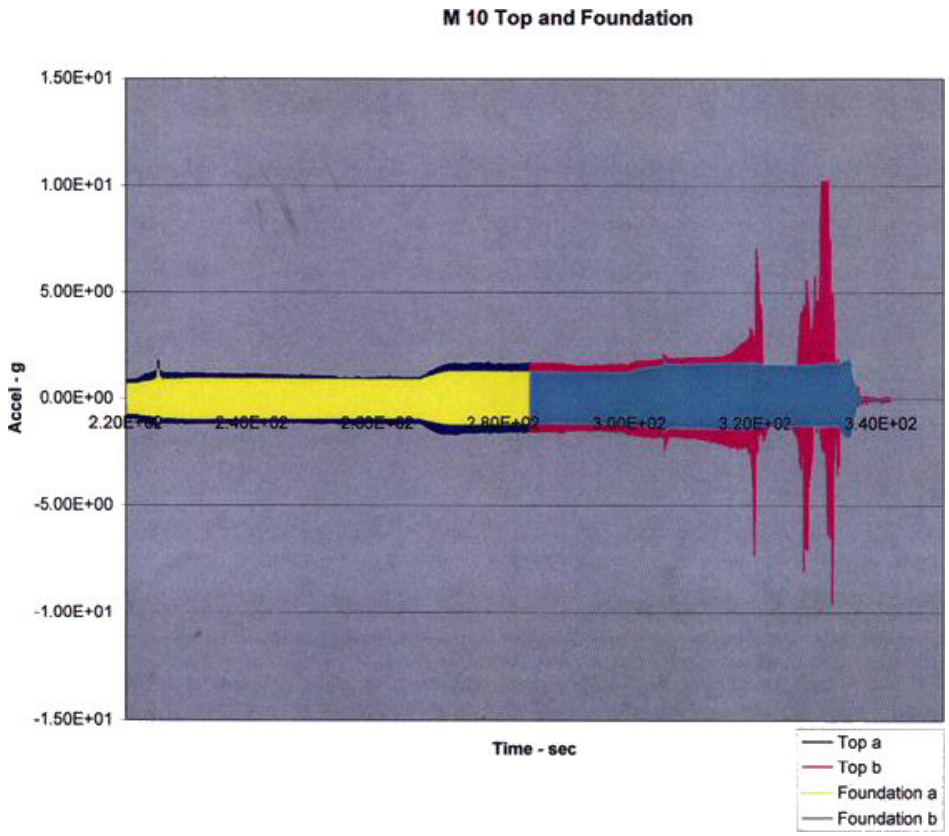

Figure 24.—Horizontal-joint model accelerations.

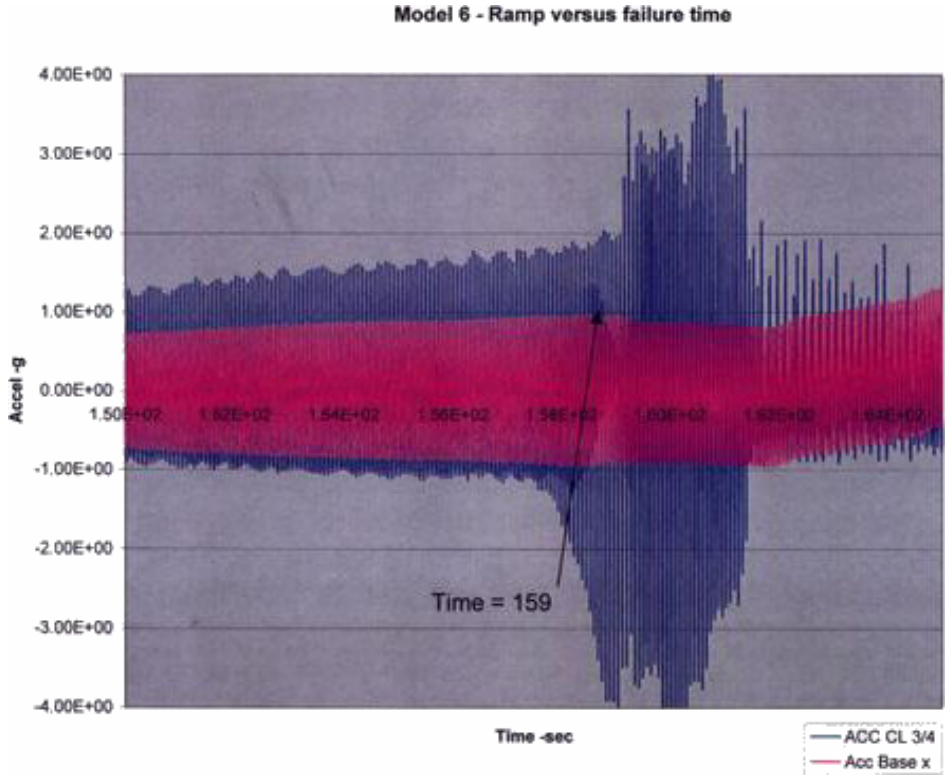

Figure 25.—Vertical-joint model accelerations.

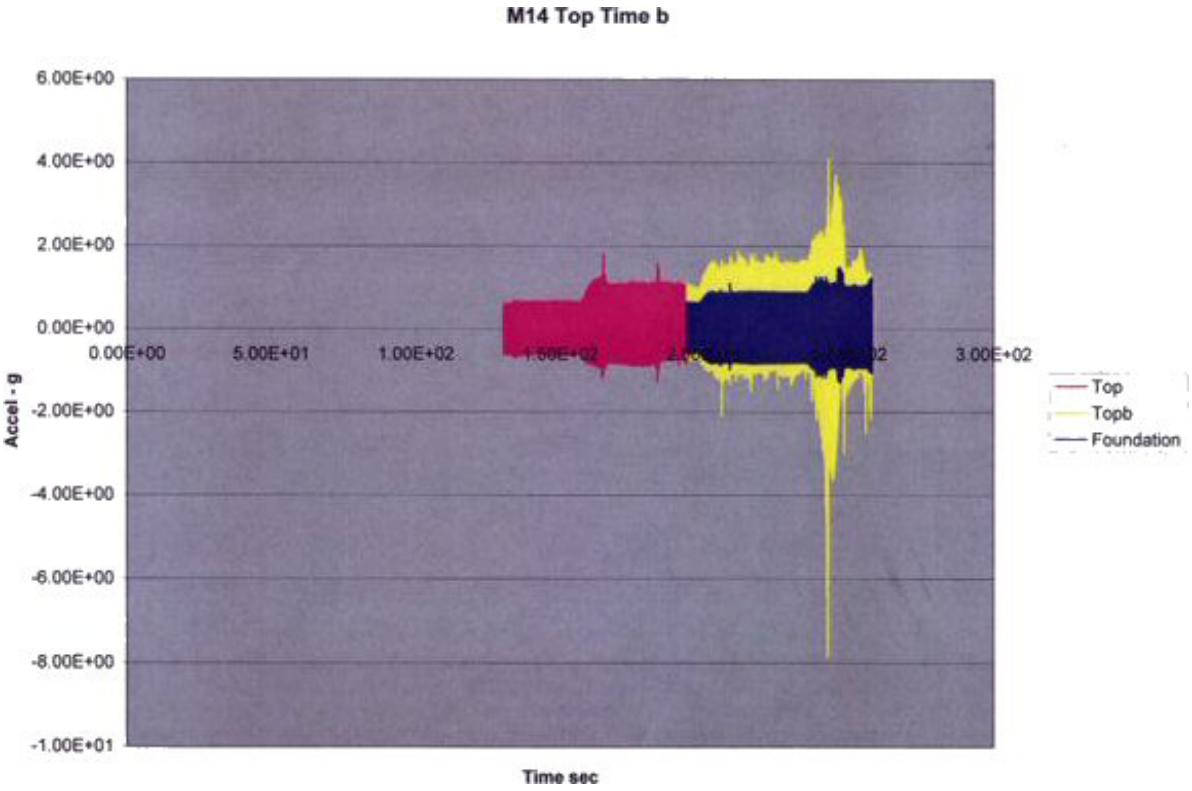

Figure 26.—17x2-joint model accelerations.

What is clear in all the figures is that there is a linear increase of acceleration with height until the initiation of cracking. When cracking occurs, this linear behavior changes rapidly. This sudden and extremely different nonlinear behavior is highly dependent on joint type as described in the next section.

An investigation of the linear effect for different types of models is shown in figure 27, with the critical, or acceleration to cause cracking, normalized to a the stiffness within each model. In this figure, it can be seen that, for this model, cracks generally occurred at an acceleration of 0.70 g. As all models are linear until the initiation of cracking, this parameter is unaffected by model type.

Effect of Joints on Nonlinear Behavior

Photos of the different models are shown in figures 28 through 31. These models employed the different jointing patterns of monolith, horizontal joint, vertical joint and multiple joint, respectively. From these figures, it is easily seen that the joint patterns have a great effect on the initial and final cracking patterns. Figure 32 shows all initial cracking patterns overlain on the same picture. The joints control the initial cracking pattern. The monolith breaks initially into one fairly large piece from approximately ¼ of the distance across the canyon, down to about the ¼ of the height, and then up the centerline. All other patterns are controlled by the joints. The vertical joint creates a deep crack along the joint, the horizontal joint forming the predominant pattern in the first crack. In the 17x2-

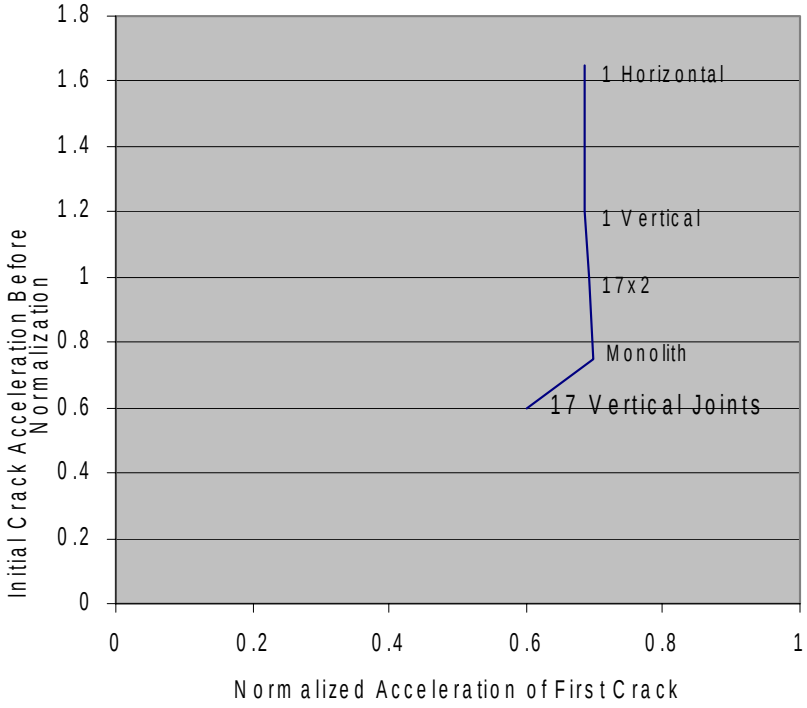

Figure 27.—Initial crack normalized to stiffness.

joint case, the upper horizontal joint forms the predominant pattern with three vertical joints in the initial pattern.

The final crack pattern is different for each model, once again showing the influence of the constructed joints. Figure 33 shows expected inflection points for typical linear analysis. Figure 34 shows the final pattern for the 17x2 model with the mode inflection points superimposed.. The pattern of the formation of five large blocks in the failure mode is somewhat common in all models and might be suggested as a pattern that is consistent with the modes of the structure. The final failure in all models occurred after considerable time, on the order of 20 to 30 seconds of shaking following the initial crack. This is consistent with comments by other authors (Niwa and Clough, 1982) and is most likely associated with the need to abrade joints before there is sufficient space for the blocks to snap through in the downstream direction.

Effects of a Wide Canyon

Figure 35 shows the initiation of failure in the dam at the ¼ point across the canyon and the centerline of the dam. Two differences are noted:

1. The onset of nonlinearity occurs first in the centerline and about 2 second later at the quarter point. Although this seems like a small difference, accounting for the time similitude of 12.8 times for the model to field, this

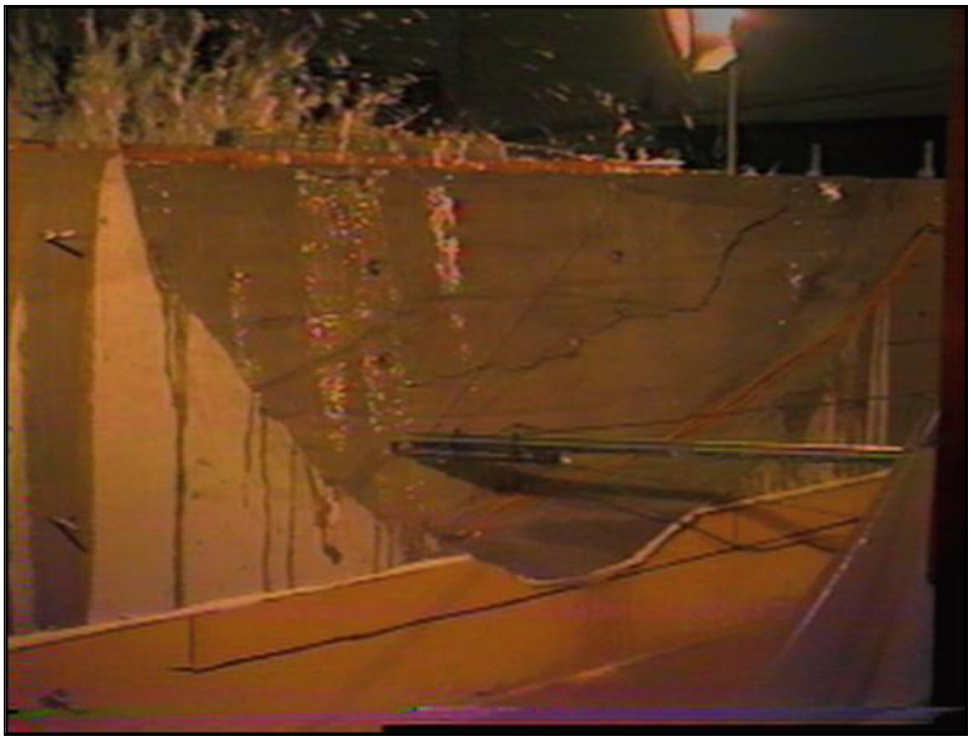

Figure 28a.—Monolithic model 2 initial cracking.

Figure 28b.—Monolithic model 2 final crack.

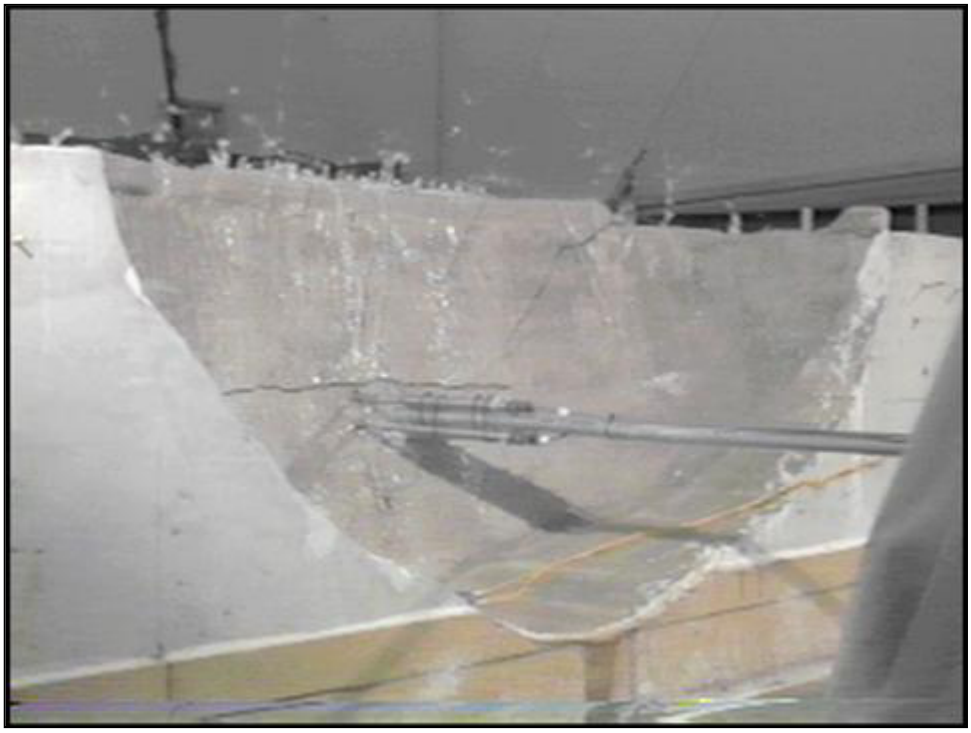

Figure 29a.—Model 10—horizontal joint initial failure, south camera.

Figure 29b.—Model 10—horizontal joint final failure.

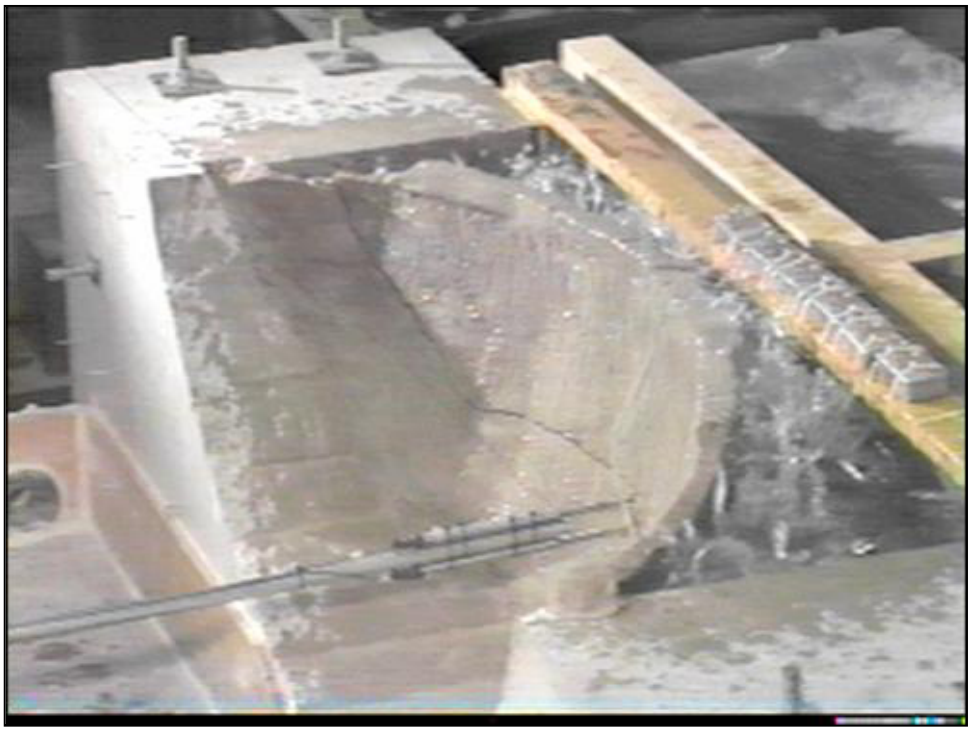

Figure 29c.—Model 10—horizontal joint north view, initial cracking.

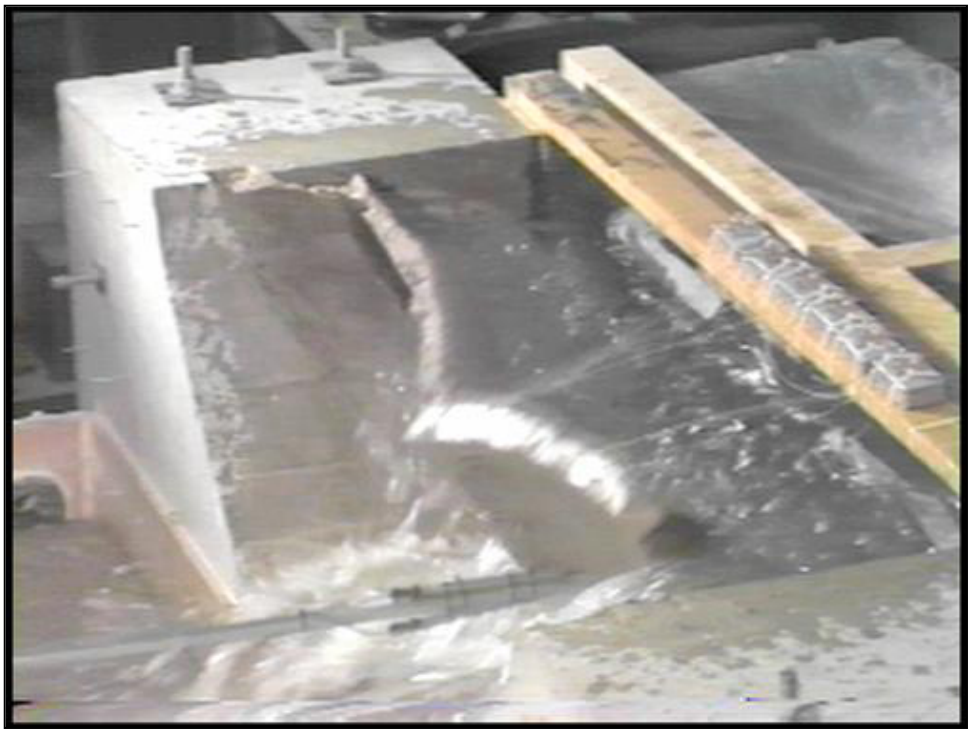

Figure 29d.—Model 10—horizontal joint north view, final failure.

Figure 30a.—Model 11—vertical joint south view, final failure.

Figure 30b.—Model 11—vertical joint south view, initial cracking.

Figure 30c.—Model 11—vertical joint north view, final failure.

Figure 30d.—Model 11—north view, initial cracking.

Figure 31a.—Model 11—vertical joint south view, final failure.

Figure 31b.—Model 11—vertical joint south view, final failure.

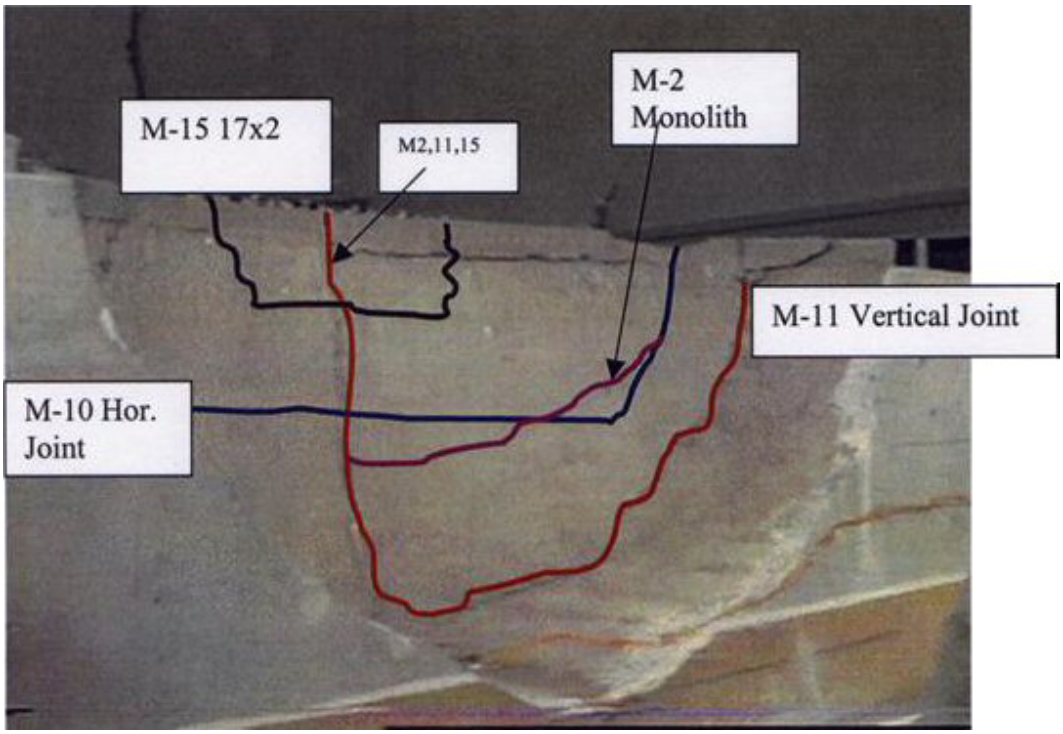

Figure 32.—Approximate location of all initial cracks in different models.

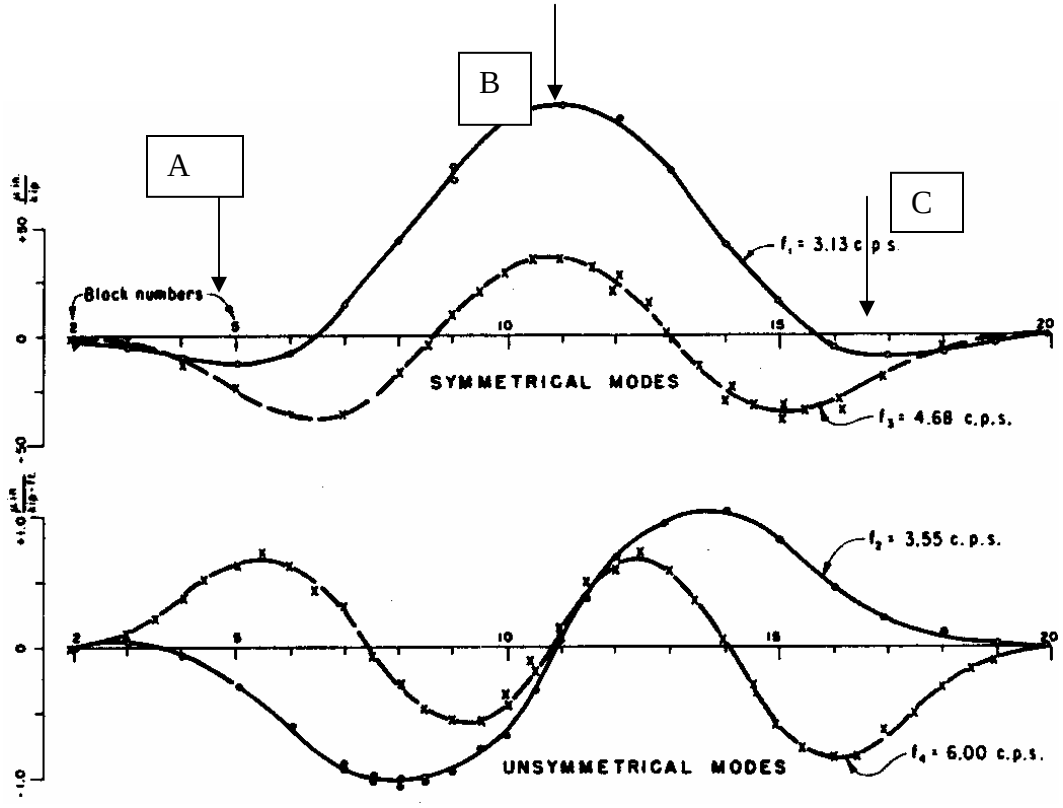

Figure 33.—Mode shapes for typical dam, measured in the field.

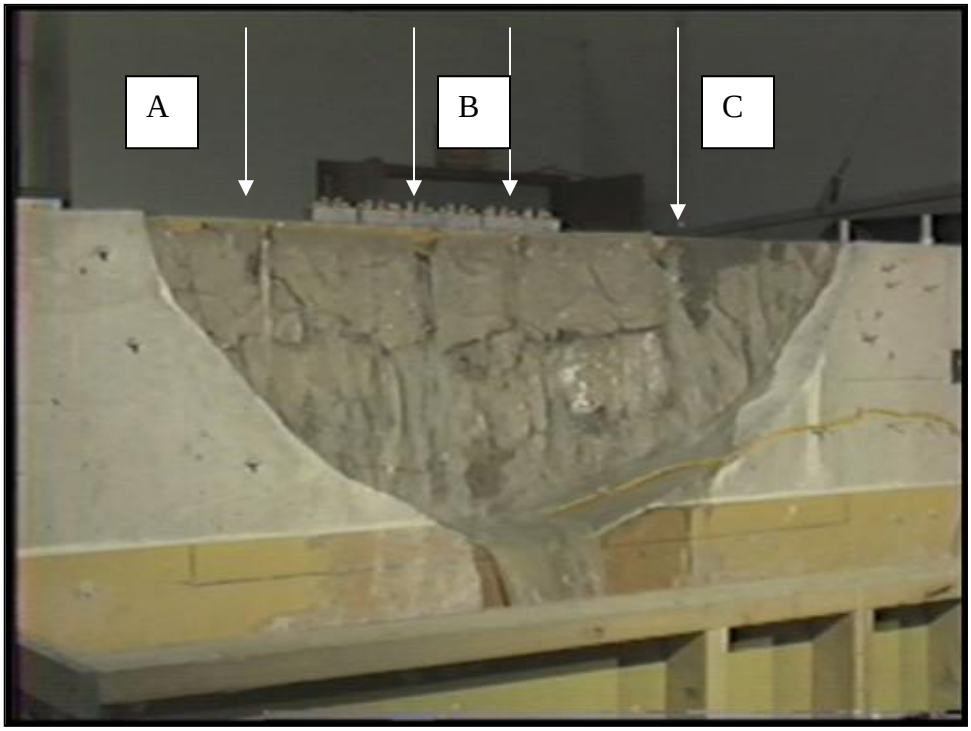

Figure 34.—Final crack pattern and mode shapes.

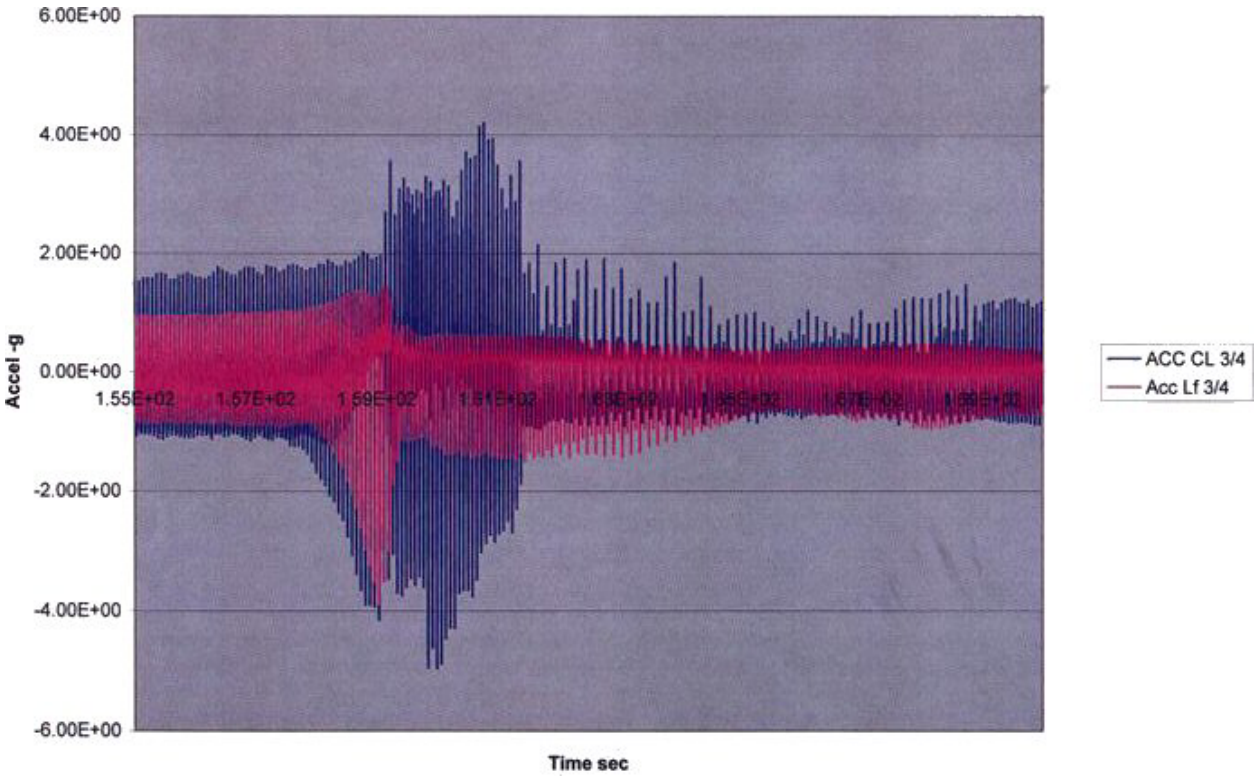

Figure 35.—Cracks accounting for wide canyon effects.

difference is 6.4 seconds later in real time, which is a significant portion of an earthquake record.

2. The degradation of the acceleration of the ¼ point is almost immediate, whereas there is a time period of approximately 2 seconds of increased motion in the centerline before the degradation of acceleration is observed.

Water in Joints

One additional issue for consideration is the ability of water to penetrate joints during the earthquake. Water was observed squirting from cracks in the dam as they opened and closed after failure. It is noted that no considerations were made to model the viscosity of the water for the model scale. Nevertheless, water is clearly seen traveling through the dam in this sequence.

Conclusions

1. The Koyna Model gave results similar to previous studies and to what actually happened in the field. The 3-D arch dam model compares with previous models and linear measurements such as response frequencies made in the field.

2. All models show the onset of sudden cracking and pronounced structural nonlinearity following cracking. This nonlinearity is characterized by the bottom of the dam being able to slip back and forth beneath the top of the dam.

3. The arch dam model demonstrates a critical acceleration of 0.70 g's for first cracking of this specific model independent of joints in the models.

4. The crack pattern in the models is dominated by the joint patterns.

5. The time to final full failure when converted to full scale times exceeds the duration of any recorded earthquake.

6. Final failure is a push through of the dam into downstream. This failure mechanism appears to require abrasion in the joint before it can be established.

7. Water does pass through cracks in the model in approximately $\frac{1}{10}$ of a second.

Recommendations

1. Physical models can be used to find extreme cases needed for the evaluation of critical structures. The results can be used to improve understanding of numerical modeling or to develop and improve capability. The results can be used to develop initial and terminal failure modes for issues such as risk analyses.

2. Some data needed for nonlinear modeling has been gathered using preliminary testing methods. Additional work is required to establish methods to find necessary parameters.

3. Wide canyon dams are clearly affected by the cross-canyon mode shapes. Some studies need to be conducted for narrow canyons to investigate the initiation of cracking and failure mechanisms.

References

Bureau of Reclamation, *Vibration Studies of Monticello Dam*, Research Report No. 9, United States Department of the Interior, 1967.

Chopra, A.K. and P. Chakrabarti, *The Koyna Earthquake of December 11, 1967 and the Performance of Koyna Dam*, Report No. EERC 71-1, Earthquake Engineering Center, University of California, Berkeley CA, 1971.

Donlon, W.P., *Experimental Investigation of the Nonlinear Seismic Response of Concrete Gravity Dams*, Report No. EERL 89-01, Earthquake Engineering Research Laboratory, California Institute of Technology, Pasadena, 1989.

Donlon, W.P. and J.F. Hall, "Shaking Table Study of Concrete Gravity Dam Monoliths," *Earthquake Engineering and Structural Dynamics*, Vol. 20, 1991, 769-786.

Duron, Z.H. and J.F. Hall, "Experimental and Finite Element Studies of the Forced Vibration Response of Morrow Point Dam," *Earthquake Engineering and Structural Dynamics*, Vol. 16, 1988.

Harris, David W., C.E. Mohorovic, and T.P. Dolen, "Dynamic Properties of Mass Concrete Obtained From Dam Lines," *ACI Materials Journal*, Vol. 97, No. 3, American Concrete Institute, 2000.

Harris, David W., Nathan Snorteland, Timothy Dolen, and Fred Travers, "Shaking Table 2-D Models of a Concrete Gravity Dam," *Earthquake Engineering and Structural Dynamics 2000*, Vol. 29, 2000, 769-787.

Houqun, Chen, et al., *Model Test and Program Verification on Dynamic Behavior of Arch Dams with Contraction Joints*, Institute of Water Conservancy and Hydroelectric Power Research, Report No. SVL-94/02, July 1994.

Krawinkler, H. and P.D. Moncarz, *Similitude Requirements for Dynamic Models*, American Concrete Institute, v SP-73, 1980.

McCafferty, R.M., *Test Facilities USBR Vibration Test System*, *Shock and Vibration Bulletin*, Bulletin 41, December 1970, 109-117.

Mir, R.A. and C.A. Taylor, "An Investigation Into Base Sliding Response of Rigid Concrete Gravity Dams to Dynamic Loading," *Earthquake Engineering and Structural Dynamics*, Vol. 25, 1996, 79-98.

Niwa, A. and R.W. Clough, *Non-Linear Seismic Response of Arch Dams*, Earthquake Engineering and Structural Dynamics, Vol. 10, 1982, 267-281.

Niwa, A. and R.W. Clough, *Shaking Table Research On Concrete Dam Models*, Report No. UCB/EERC 80-05, Earthquake Engineering Research Center, University of California, Berkeley, CA, 1980.

Norman, C.D., *Dynamic Failure Tests and Analysis of a Model Concrete Dam*, Technical Report SL-86-33, U.S. Army Waterways Experiment Station, Vicksburg, MI, 1986.

Oberti, G. and A. Castoldi, "The Use of Models In Assessing the Behavior of Concrete Dams," Dams and Earthquakes—Proceedings of a conference held at the Institution of Civil Engineers, London on 1-2 October 1980, Thomas Telford Limited, London, 1981.

Oberti, G. and E. Lauletta, "Structural Models for the Study of Dam Earthquake Resistance," Ninth International Congress on Large Dams, Istanbul, Turkey, Sep. 4-8, 1967.

Plizzari, Saouma, and Waggoner, "Centrifuge Modeling and Analysis of Concrete Gravity Dams," *Journal of Structural Engineering*, Vol. 121, No. 10, October 1995, 1471-1479.

Renzi, Ferrara, and Mazza, *Cracking In a Concrete Gravity Dam: A Centrifugal Investigation*, International Workshop on Dam Fracture and Damage, Chambery, France, 1994.

Rouse, George C. and Jack G. Bouwkamp, *Vibration Studies of Monticello Dam*, Research Report No. 9, Bureau of Reclamation, United States Department of the Interior, 1967.

Takahashi, T., *Results of Vibration Tests and Earthquake Observations on Concrete Dams and Their Considerations*, ICOLD Congress No. 8., Edinburgh, Report 14, Vol. II, 1964, 239-260.

Tinawi, R., P. Leger, M. Leclerc, and G. Cipolla, *Shake Table Tests for the Seismic Response of Concrete Gravity Dams*, Eleventh European Conference on Earthquake Engineering, Paris, September 1998.

Yoshida, T. and K. Baba, "Dynamic Response of Dams," *Proceedings of the Third World Conference in Earthquake Engineering*, Auckland, Vol. 2, 1965, 748-764.

Appendix

Summary Paper:

Investigation of the Failure Modes of Concrete Arch Dams Using Physical Model Tests, by David W. Harris and Fred Travers

Investigation of the Failure Modes of Concrete Arch Dams using Physical Model Tests

By
David W. Harris[1], Fred Travers[2]

Summary

This paper describes the design and testing of physical models of concrete arch dams. The models are approximately 1/150 scale of a typical wide canyon dam. Material properties are adjusted to the model scale, a reservoir and foundation are included. The models utilize different joint patterns of a monolith, single horizontal and vertical joints, and multiple vertical and horizontal joints. Models are tested to collapse of the structure. Conclusions are that initial behavior of the structure is not influenced by the joints. Initial cracking of the models is influenced by the joints. Final collapse is a push through of sections of the dam downstream and is controlled by the joints both with the pattern of the failure and with the acceleration required to fail the structure. Water was observed passing through the model during the loading.

[1] Group Manager, Materials Engineering and Research Laboratory
U.S. Bureau of Reclamation, D-8180
PO Box 25007
Denver, CO 80225

303-445-2375 Phone
303-445-6341 FAX
Email: dwharris@do.usbr.gov

[2] Electronics Engineer, Materials Engineering and Research Laboratory

Key Words: Concrete dam, Earthquake, Physical Model, Arch dam, Failure

I. Introduction

The earthquake event in 1967 and subsequent cracking of Koyna Dam led to advanced studies of dams and the effects of large loads.[1] Pacoima Dam showed a opening in a contraction joint of nearly a centimeter following the San Fernando Earthquake of 1971[2]. Following the Northridge Earthquake in California on January 17, 1994 and the Kobe Earthquake in Japan 1 year later on January 17, 1995, new consideration has been given to the magnitude of the vertical acceleration of seismic events. Additional damage occurred in the Pacoima Dam along the abutment of the dam in the Northridge Earthquake. An extensive overview of work done in the investigation of dam performance, dam properties based on field observations, and laboratory testing was presented by Hall in 1988[2]. The field reference values from this work are used in this study to configure parameters for a physical model. Continuing concerns about the performance of concrete dams subjected to severe earthquakes has motivated investigation into ways to analyze and predict this performance using both physical modeling and nonlinear numerical analysis techniques[3].

Previous model studies of the behavior of concrete dams subjected to seismic accelerations have been conducted on gravity dam monoliths[3,4,5,6]. In references 3 and 4 attention was given to developing a modeling material which maintained similitude with the prototype. In this paper a new modeling material is suggested for models on the scale of 1/150. More recent studies have been completed as centrifuge models[7,8]. In the centrifuge model of Toktogul Dam[9] cracks appeared along the abutments of the model and along a horiziontal line similar to the results which are found in this paper.

Arch dams have also been tested as physical models. The arch section of the Techi Dam, Taiwan has been modeled at a scale of 1/150[4]. A primary purpose of that study was to model the opening of joints, thus the dam was articulated. The model was tested with motion in 2 axes, upstream/downstream and cross-canyon. Vibration mode frequencies were tested by suspending a weight from the model and subsequently cutting the weight loose to produce face vibrations. The El Centro Earthquake record was used in the shake table model test with a time reduction of $\sqrt{1/150}$. Intensity was increased until the model collapsed. Significant joint degradation occurred at the arch end, probably due to crushing of the material at the end. In biaxial excitation the arch collapsed with 1.34 g acceleration in the upstream/downstream direction and 0.91 g in the cross-canyon direction. The collapse occurred close to the end of the excitation. It was noted[10] that the test results showed significant non-linear behavior. Significant influence of the joints generated increasingly poor correlations with the numerical analysis. A method to account for crushing in joints was suggested to improve the analytical results. The physical model in this study included joints as discontinuities. The input motion is sinusoidal, with collapses being induced by an increase in the intensity of the record. As stated in this paper, collapses occurred near the end of the testing record, similar to the previous study.

Other failure tests of models[11] have been conducted with shake tables at a scale of 1/100. A sinusoid input motion was used to determine characteristic frequencies of the structure. Next, similitude-corrected time histories of seismic events were used at increasing amplitudes to induce failure. Natural frequencies appeared to be produced correctly when the foundation was carried 1 to 2 times the height of the dam both depth- wise and in the lateral directions. The length of the reservoir showed no significant effect with reservoir length being 2 times the dam height. Fot the

models in this study a rigid (stiff) foundation is used which does not represent the field case. However, the frequency contact does appear to match the field case. A reservoir is included with the length of about the depth of the reservoir; a dissipating wall was used to reduce reflection effects.

Another model[12] study was the Futatsuno Arch Dam. This 76 m high, 210 m crest dam was modeled at 1/50 scale. In this model the first crack appeared at 0.27 g and 32 Hz in a spillway pier. On the dam cracking initiated at 0.41 g and 30 Hz. Final collapse occurred at 0.69 g, and 17 Hz. Accelerations which induce failures are similar in this paper. Models have also been tested at the ISMES facility in Italy[11,13].

A series of Experimental Investigations was conducted by Zhou, et al[14], to investigate high arch dams. The model scale of 1:350 was used with a modeled compressive strength material of 0.3 Mpa (45 psi), or 15,750 psi in the field case. Joints were modeled and were formed by cutting the mold with a thin saw and using asphalt pads in the joint. The softness of the joint padding was shown to have an effect on the response of the model. Final cracking patterns were shown to be influenced by the joints, with a monolithic dam showing cracking in the uppermost part of the dam, and jointed models showing cracking deeper in the dam. The model reported in this paper uses a model material with a simulated field strength of approximately 34 Mpa (5,000 psi). Joints are cast into the model in various patterns, creating various versions of tests similar to this reported case. Water is used in a reservoir behind the modeled structure. The relationship of crack locations is similar to this reported case.

Testing has been completed to model sliding of dams on the foundation contact only[15]. Typically, these models were 1000 mm in height and had a short reservoir tank (0.4 m in length) with absorbent rubber to eliminate the hydrodynamic effect. The input motions used were: a) a 7.5 Hz. sine wave (this waveform was hard to match exactly because some free vibration was present in table), b) a 5 Hz sine wave ramped up in 5 cycles, held for 10 cycles, then ramped down in 5 cycles, c) simulated earthquake of 12 seconds duration with the input amplitude ramped until slipping occurred. The input motion used in the models in this paper uses a ramped approach to increase the acceleration to failure, each load is held 30 seconds and then ramped by 0.25 g's.

The purpose of the investigation described in this paper is to produce failures in arch dam models for comparison with predictions by nonlinear computer models[16,17]. Unlike many of the previous investigations, a specific field site is not being modeled using precise similitude relationships. Rather, lowest value properties, and worst case loadings are allowed and the model is loaded to absolute collapse in the test. The models were designed to the extent possible to maintain similitude relationships of typical properties found in field tests, and in standard laboratory tests, and yet be simple enough for direct comparison with the computer-predicted results. This testing was conducted at the Bureau of Reclamation, Materials Engineering and Research Laboratory[18]. This paper attempts to describe in detail the physical modeling, the material properties of the models, similitude comparisons, and the models' behavior. The computer predictions and comparisons with these physical models have already been published[17,18]

II. Experiment Overview

All of the models chosen for this study were based on a similar geometry. The field case selected was a typical arch dam of approximately 90 m. (300 feet) in height in a wide canyon. The scale chosen for this model series was 1/150. A model that was 0.6 m (2 feet) in height, with a cross canyon width of 1.7 m. (5 feet 6-1/2 inches) was constructed on a 1-dimensional (upstream-downstream) shake table . The arch was constructed as a single curvature arch with a vertical upstream face and tapering with increasing height. A reservoir was constructed behind the dam and filled with water for the tests. At the initiation of shaking the reservoir height was approximately 1.2 cm (1 inch) from the top of the dam.

Different models were constructed: 1) A monolithic dam, 2) One horizontal joint at approximately mid height, 3) One vertical joint at the mid point of the model dam, and 4) 17 vertical joints and 2 horizontal joints (one model was run with17 vertical joints as a test of construction method), see Table 1. All models were run with a sinusoidal input motion at 14 Hz beginning at 0.25 g and increasing every 30 seconds by 0.25 g until a structural collapse was created in the model.

III. Similitude considerations

Considerable effort was made in the early model considerations to match each property in the model using a similitude modeling approach. Early in the material development it was clear that it would be difficult to model all parameters with a perfect similitude match. For that reason, the following priority of modeling considerations was made: 1. Failure mechanism, 2.

Tensile strength, 3. Frequency content, 4. Strain rate, 5. Compressive strength, 6. Modulus, 7. Density. Table 2 summarizes the model similitude comparisons.

Creating a modeling concrete which failed in the same manner as the full strength field case was considered the most important modeling consideration. This was due to the desire to allow failure through the dam, and not assume *a prior* that all cracks occur in joints. For the monolithic dam, any failure mechanism would be initiated as a material failure, as no joints are present. In the models with only horizontal, or vertical joints, a collapsing failure would also require failure through the material. In the models combining vertical and horizontal blocks, it was possible for large blocks to form from combined joints and fail, but the possibility of a material failure instead of a failure through the joints only was made possible in the model with a modeled material. Thus, a modeling material which simulated full scale behavior was developed.

The comparison of failure mechanisms in concrete was made by comparing the shear failure produced in a compression tests. Direct tension failures, which occur on a flat plane, were not tested but were assumed to occur in a typical flat plane based on the similar nature that beam tests which were run failed in the same manner of full strength mixes. That is, the beams failed in a vertical plane. Split cylinder tests also were identical in their failure mechanism. A typical failure, in compression, is shown in figure 1. On the left is a failed cylinder from the model mix, while a typical 50 year old cored sample is shown on the right. Note that a typical shear plane of approximately 65 degrees is shown in both failures. That is, the plane of failure that occurs in shear, in both the model mix and a typical full strength, aged concrete core occur in the same manner.

Properties of mass concrete in dams has previously been published[19,20]. These results represent tests run from approximately 500 cores obtained from dams and used to find various standardized properties. All tests were run in accordance with ASTM[21] C39 - Standard Test for Compressive Strength of Cylindrical Specimens, ASTM[21] C 469 Standard Test for Modulus of Elasticity and Poisson's Ratio in Compression, ASTM[21] C496 Splitting Tension Strength of Cylindrical Concrete Specimens. Tests for Dynamic Properties were done using similar procedures and were tested at strain rates appropriate for earthquake loadings (see later discussion) owing to the rate sensitivity of concrete. It is not suggested that these are the only properties that can be measured from core, only that these standard methods serve as a comparison of other properties reported in the literature. For this model study, values of properties from the model mix, as measured, are compared to properties which have previously been measured from dam cores. One additional standard test was used, the Three-point bending test - ASTM[21] C-78, with specimens cast into standard beam molds from the model mixed material.

The compared material property values and a ratio to compare similitude ratios are shown in Table 2. Tensile strength was considered high in importance to assure that failures initiated in a loading range similar to field cases. Values of split tension strength range in the model mix from 20 to 33.3 kPa (3.09 to 4.83 psi), with an average value of 28.3 kPa (4.1 psi). The range in the model mix is approximately 35%; this range of values is less than a typical range of values tested from cores obtained from existing dams and tested in the lab using the split cylinder test (see Table 2). A lower range is considered a positive in the research environment to lower the parameter variation. The average value of 28.3 KPa (4.1 psi) if scaled to the prototype using a value of 150 would represent a prototype tension strength of 4.24 MPa (615 psi). Values

obtained from core recovered from operating dams range from 1.5 MPa (215 psi) to 5.4 MPa (785 psi). This modeled value of tension strength is well within this range of measured values and therefore is considered to represent a proper value within similitude considerations as shown in Table 2.

Compression strength of the mix was considered a lower priority for these simulations. The average value for compression strength, as shown in Table 1 is 0.2 MPa (31 psi). Scaled by the model ratio of 150 this would produce a modeled value in the field of 32 MPa (4650 psi). Values measured from cores obtained from dams range from approximately 9.6 MPa (1400) psi to 58 MPa (8400 psi). An average of all core tested is 30.5 MPa (4425 psi). Thus this parameter is considered in the range and near the average of all tests completed and a proper value within similitude considerations, as shown in Table 2.

The average Modulus of Elasticity for the model mixes as shown in table 1 was 23.5 MPa (3415 psi). This value scaled by the model scale of 150 would compare to field values of approximately 3620 Mpa (525,000 psi). The lowest measured Modulus of Elasticity measured from core taken from dams is 5170 MPa (750,000 psi). Thus, this parameter does not fall within values from the field, being 0.7 of the lowest measured value or 30% less than a perfectly modeled similitude parameter, this is noted in Table 2. The lower Modulus would result in larger displacements, and higher strains, under dynamic loading than would be expected in the field. Thus failures reported in this study may occur at lower, or more conservative loads. Comparisons with numerical predictions which use the measured values as input into the numerical models can still be compared directly.

The average density for the modeling mix was 1890 kg/m^3 (118 lbs/ft^3). Reclamation data[22] for average weight of fresh concrete varies from 2250 kg/m^3 (141 lbs/ft^3) with a 3.8 cm. (1 ½ inch) MSA (Maximum size of aggregate) and 4.5% air content to 2515 kg/m^3 (157 lbs/ft^3) with 15 cm. (6 inch MSA) and 3% air content. Density is not a parameter which is scaled and therefore should fall into this range. The density of the model mix does not fall into this range, it shows a ratio of 0.85 from the reference minimum value, or about 15% low from measured field values, as noted in Table 2.

The frequency content of an earthquake when loading a dam dynamically plays an important role, as the structural responses that can be excited produce a more critical situation. A typical earthquake spectrum used in dam analysis is shown in figure 2. Values of modal periods for a typical dam[2] (which is similar to this model) tested in the field using a shaker device are superimposed on Figure 2a. A reference line has been added to show that the first principle period in the earthquake spectrum would relate to the lower mode shapes of the dam, in this case the spectrum would occur near the 3rd mode shape of the dam. The modal periods for the model were calculated using a finite element analysis. These modal periods are shown in figure 2b, along with a reference line which represents the input motion of a 14 Hz. sinusoid. Comparing the two figures it can be observed that the frequency content of the model input excites most closely the 3rd modal frequency (see reference line)and is similar to the first period motion in the field situation which excites the structural frequencies between the second and third structural frequencies. This comparison demonstrates that the frequency content in the model and field cases are similar, as noted in Table 2.

The advantages of using a sinusoidal input have been discussed previously[23]. With a regular input pulse, the onset of nonlinear behavior may be detected in the instrument measurements before the effect is visible in the model. Figure 3 shows the instrument readings for the model with one horizontal joint. In this graph the base accelerations of the model are plotted in white (on a white background) which for clarity in the figure masks the accelerations of the accelerometer at the 3/4 height position on the model (plotted in black). From the figure it can be seen that initially the accelerations in the upper part of the dam grow with the input motion in the first part of the record. The onset of nonlinear behavior is seen at approximately time 317 seconds in the record; there is a shift in the record from centering around zero. At approximately time 320 seconds in the record, the accelerations begin to grow rapidly and a spike in the record indicates when the crack in the model cracks passes through the model cross section. It is this time when the failure is visible to the eye, about 3 seconds after the effect begins. Following the crack, the top motion can not keep up with the base, in other words - the base can slide back and forth under the top, and the acceleration is masked in the graph by the foundation motion plotted in white. Following time 330, the acceleration is increased, as per the test protocol, and as can be seen the collapse of the structure occurs as indicated by the high accelerations and erratic behavior of the instruments.

As mentioned, the strain rate to which the model material was subjected during loading was given a high priority in the modeling considerations. This is due to the inherent increase in concrete's strength at failure, as the strain rate is increased. An earthquake record produces a typical strain rate for concrete of 10^{-3} (inches per inch per second)[24]. Data from cores taken from actual dams and tested at a strain rate of approximately 10^{-3} showed a compression strength ratio of increase from static to dynamic strength of 1.07 and a increase of tension strength of

1.44. Data from other tests[25] suggest an increase of 1.1 for compression strength in the same order strain rate, and 1.56 for tension. At an order higher strain rate (10^{-2}) data[25] suggests an increase of 1.15 for compression and 1.7 for tension. For computation purposes[26], a generally linear trend of approximately a 10% increase in strength for each order of magnitude increase in strain rate. The strain rate comparison from field cases to the model was made by comparing a typical earthquake strain rate of 10^{-3} in the field to an estimated strain at failure(tension), 0.0001 in the model, at a frequency of 14 Hz; yielding a strain rate of 1.4 10^{-3} which would yield an expected increase of 4% in strength due to an increased rate effect. As the strain at failure is conservatively estimated, the strain rate is believed to be accurately modeled. An increase in the speed of the time history plot using a similitude ratio for time of the square root of the scale (150) would yield a time suppression ratio of 12.25. This increase would result in a corresponding apparent increase in tension strength of about 12.25%. Although this additional strength resisting failure would be within a reasonable range of tension strength values actually measured from cores retrieved from dams, it may lead to nonconservative assumptions as the dam will not fail until higher loads are reached, relative to a slower strain rate.

Summarizing the model to measured data comparisons: The modeling material fails in the same shearing manner as the field material, the frequency content is similar in the field and model cases, the strain rate effect is a possible increase of approximately 4% in the tension strength, the model static tension and compression strength values demonstrate similitude ratios within the range of expected variation from cores measured from dams, the Modulus value is approximately 30% lower than measured values - which will allow greater displacements and

strains at lower loads, the density is approximately 15% low compared to laboratory measured values of fresh mixes.

IV. Concrete Mix Design

For this study a new low-strength concrete mix was designed. Considerable work in this area has been accomplished in previous studies[3,4,11] to produce a similitude-appropriate concrete mix. Work with 2 dimensional model studies here in the same laboratory and the advantages of this mix design are discussed in reference 23. This mix design was modified for the 1/150 scale models of this study. The mix components and proportions are shown in Table 3.

Preparation of the mix required special care due to the need to saturate the bentonite in the mix. Bentonite and water for the mix were placed in a paddle mixer and mixed continuously for approximately 5 hours. When the mix appeared visually to be smooth and consistent, the remaining ingredients were added, mixed for a period of a few minutes. The mix was emptied into containers suitable for forklift transport and poured into the model mold immediately. The shake table was used to vibrate the mold slightly with a few strokes 2 or 3 times as the mold was filled. Any type of vibratory device or tapping of the mold had been eliminated in previous experiments as this changes the water/cement ratio due to bleeding in a material this weak and causes a change in strength.

As was noted with Table 1 and the above discussion, properties were obtained from each mix for the different models to be used as input when numerical methods were attempted as a

comparison to the model results. A direct measurement of the damping characteristics was not attempted due to the fact that the model shape was difficult to suspend independently, the mechanical effects of the table are difficult to isolate, and the material was weak for such a test. Some early attempts were made using an input amplitude of 0.05 g's to measure and predict modal frequencies. Although this loading was quite low, 2 models were lost as the motion was hard to energize at this low level.

V. Model Construction, Loading, and Instrumentation

The bottom thickness of the arch was 17.75 cm. (7 inches) with the top thickness being 2.54 cm. (1"). Each model was poured using a form to produce the arch shape. Figure 4 shows one model ready for testing (note that the reservoir is covered with plastic behind the dam).

The dam model was made of a modeled concrete material and was placed into an abutment made of concrete of 27 MPa (4,000 psi) compression strength. The abutment was the same height as the arch with heavily reinforced blocks on each side which extended a total of 56 cm. (22 inches) in the upstream/downstream direction and were 35 cm. (14 inches) wide from the dam interface to the edge of the model. The foundation was approximately 13 cm. (5 inches) thick at its thinnest location in the center of the dam. All thread rods which were 2.54 cm (1") in diameter were used to securely fasten the abutment block to the shake table. The modeling intent was to produce a foundation that was rigid relative to the dam. This simplified the direct comparison of numerical prediction results[17,18] since nonlinear material modeling was not necessary in the foundation An offset key was used in the foundation to receive the model.

Joints when used in the model were made horizontally by placing 1 layer of sheet plastic on top of a lift and then proceeding to pour. Vertical joints were constructed using a bag of plastic (2 layers) with a rubber strand on the downstream sloped face. The rubber strand was pulled tight to force the plastic bag against the face. A forsenic piece of a model is shown in Figure 5 to show the joints in a failed and nonfailed portion of the dam (showing the bags). Note the horizontal line on the concrete in the model which points out the horizontal joints, and that failure did not occur in the joint plane but through the modeling material.

The upstream extent of the reservoir from the dam was approximately 0.76 m.(2.5 feet), or slightly more than 1 dam height. The reservoir was constructed on the shake table and thus was inflight with the model. A gravel wall was used at the upstream wall to aid in dissipating energy and reflecting it back into the reservoir and towards the dam. The reservoir fluid was plain water, it was applied directly to the upstream concrete face of the model.

For these experiments a shake table was constructed having movement constrained to a single axis (horizontal only in the upstream/downstream direction). The table was tested for its response modes and also tested in motion with accelerometers to determine its capabilities for use at higher frequencies. The table responded well for input frequencies below 22 Hz, which was below the table's measured lowest natural frequency of 30 Hz. Higher frequencies were eliminated for testing. Response of the table was clearly best at frequencies of 26 Hz and below. A sinusoidal input motion was easily applied within these limitations.

Instrumentation in all models consisted of accelerometers on the base of the dam and at 1/4 points throughout the height of the dam at the centerline, and at the predicted[2] inflection points along the length of the dam. In earlier models, LVDT's were used downstream in the same locations as the accelerometers on the centerline; these were later abandoned to assure that the push through of the final failure was not braced or influenced by the instruments. A highly accurate pressure gage was submerged upstream of the dam in early models but did not register any hydrodynamic pressure changes and was later abandoned.

VI. Results and Indications of the Models

The models all acted in a structurally linear manner until the onset of any cracking. This was evidenced by a characteristic mode shape and increase of acceleration from the base of the dam to the top of the dam. As noted in the discussion previously, this is shown in Figure 3. This pattern was shown for the Monolith, Horizontal-Only Joint, Vertical-Only Joint, and 17x2-Joint models.

Figure 5 shows all initial visible cracking patterns overlaid on an outline sketch of the model. Initial cracks appear in the video of the model test in a single frame, that is the crack becomes visible in 1/30 of a second. The joints control the initial cracking pattern. The monolith breaks initially into one fairly large piece starting approximately 1/4 of the distance across the canyon, down to about the 1/4 of the height, and then up the centerline. As noted in Table 1, this initial crack occurs at an acceleration of 0.75 g's. (Note that all model results are shown in table 1, two of the monolithic models were lost attempting modal sweeps to measure

structural frequencies of the dam; these models are noted as " 1st pulse" in the table). The first crack in the horizontal joint only model is along the horizontal joint and along the abutments to the top of the dam. Model M-10 had a Modulus value significantly different from other models, and the acceleration of first cracking is higher and discounted from this discussion. Model M-9 showed a first crack at acceleration of 0.95. The model with a single vertical joint creates an initial deep crack along the joint and then cracks along the abutment to the top. Four vertical joint models were completed, since M-6 created a failure mode which was not typical of all other models it is discounted from the conclusions. Models M-7, M-8, and M-11, which all failed in a similar manner, are used to draw conclusions.. These models initially cracked at an approximate acceleration of 1.5 g's (with M-11 being slightly different at 1.2). In the 17x2 joint case, the upper horizontal joint forms the predominant pattern along with 3 vertical joints in the initial crack.. The initial acceleration at cracking is an average of 0.82. The variation of initial crack accelerations 0.75 to 1.5 for all cases used for conclusions is related to the variation of the model material properties in the production of each model. A modulus range of E=2302 to E=3948, a 42% difference in material property creates, a nearly corresponding 50% difference in predicted acceleration, with higher moduli or strength resulting in higher accelerations. The models generally act in a similar manner before the onset of cracking.

Models with 17 vertical joints only failed at the lowest acceleration, an average of 0.55. In these models Modulas is similar to other cases, but the split tension strength is lower which may account for the lower acceleration to initial cracks.

The final crack pattern is different for each model, showing the influence of the constructed joints, see Figure 6. The final failure of the monolith, Figure 6a was the formation of 5 predominant blocks and a subsequent downstream "snap through" of the centermost 2 blocks (this failure mode is similar and may be more clearly seen in Figure 6c). Along the lower part of the model a shear plane was formed through the dam to create the final failure. The final failure of the single horizontal joint produced a similar pattern to the monolith but the lower portion of the final crack was located on the preexisting joint (Figure 6b) and the plane of failure was along the preformed joint. The single vertical joint final failure, Figure 6c, produced cracks almost to the bottom of the model and again demonstrated 5 predominant blocks in the final failure, a shear angle was present in the failure plane in the lower portion of the dam. The model with 17 vertical joints and 2 horizontal joints failed in a pattern of 5 blocks above the upper horizontal joint, and some cracking along vertical joints between the upper and lower horizontal joint (Figure 6d). These latter failures occurred through the material rather than the joint, as shown in Figure 5. The final accelerations in Table 1 show that only the monolithic model required a significant increase in acceleration to create the final collapse. Most models failed by continuing the sinusoidal input once the model had cracked.

This testing series suggests that any significant joint will influence the final failure acceleration value when compared to a monolith. As shown in Table 2 the monolith failed at 5 g's, the horizontal crack at approximately 1.7 g's, the vertical joint only at 1.5 g's, and the 17 vertical by 2 horizontal joint model at an average of 1.0 g's. Generally more significant joints lower the final failure acceleration. The final failure in all models occurred after considerable time, on the order of 20-30 seconds of shaking following the initial crack. This is consistent with

comments by other authors[10] and most likely results from the need to abrade joints before there is sufficient space for the blocks to be pushed downstream by the water in the reservoir.

VII. Water in Joints

One additional issue for consideration is the ability of water to penetrate joints in a dam during an earthquake.. It is noted that the fluid used is water, without adjustment for viscosity similitude. Nevertheless, water was clearly seen traveling through the dam in these tests during the onset of cracking and throughout the test duration.

VIII. Conclusions

1. Models act linearly before the onset of cracking.

2. All models show the sudden onset of cracking followed by pronounced structural nonlinearity. This nonlinearity is characterized by the bottom of the dam being able to slip back and forth beneath the top of the dam.

3. The crack pattern in the models is dominated by the joint patterns.

4. The time to final failure when converted to full scale times exceeds the duration of any recorded earthquake. In this paper final failure is defined as a total collapse; note that significant cracking does occur before the final collapse.

5. Final failure is a push through of sections of the dam downstream. This failure mechanism appears to require abrasion in the joints before it can occur.

6. Water does pass through cracks formed in the model by shaking.

IX. Acknowledgments

This research was sponsored by the Dam Safety Program, U.S. Bureau of Reclamation.

X. REFERENCES

1. A.K. Chopra and P. Chakrabarti, “The Koyna Earthquake of December 11,1967 and the Performance of Koyna Dam,” Report No. EERC 71-1, Earthquake Engineering Center, University of California, Berkeley, CA 1971.

2. Hall, J.F., “The dynamic and earthquake of concrete dams: review of experimental behaviour and observational experience,” Soil Dynamics and Earthquake Engineering, Vol. 7, No. 2, pp58-121.

3. W.P. Donlon and J.F. Hall, “Shaking Table Study of Concrete Gravity Dam Monoliths,” Earthquake Engineering and Structural Dynamics, Vol 20, 769-786 (1991).

4. A. Niwa and R.W. Clough, “Shaking Table Research On Concrete Dam Models,” Report No. UCB/EERC 80-05, Earthquake Engineering Research Center, University of California, Berkeley, CA, 1980.

5. C.D. Norman, “Dynamic Failure Tests and Analysis of a Model Concrete Dam,” Technical Report SL-86-33, U.S. Army Waterways Experiment Station, Vicksburg, MI 1986.

6. R. Tinawi, P. Leger, M. Leclerc, and G. Cipolla, “Shake Table Tests for the Seismic Response of Concrete Gravity Dams,” Eleventh European Conference on Earthquake Engineering, Paris, September 1998.

7. Plizzari, Saouma and Waggoner, “Centrifuge Modeling and Analysis of Concrete Gravity Dams,” Journal of Structural Engineering, v 121 n 10, p. 1471-1479, Oct. 1995.

8. Renzi, Ferrara, and Mazza, “Cracking In a Concrete Gravity Dam: A Centrifugal Investigation,” International Workshop on Dam Fracture and Damage,” Chambery, France, 1994.

9. Lyatkher, V.M., Kapstan, A.D., Semenov, I.V., “Seismic Stability of Toktogul Dam, Hydrotechnical Construction, No.2, pp 8-14, 1977.

10. Niwa, A. and R.W. Clough, , “Non-Linear Seismic Response of Arch Dams,” Earthquake Engineering and Structural Dynamics, Vol. 10, 267-281, 1982.

11. Oberti, G. and A. Castoldi, “The Use of Models In Assessing the Behavior of Concrete Dams,” Dams and Earthquakes - Proceedings of a conference held at the Institution of Civil Engineers, London on 1-2 October 1980, Thomas Telford Limited, London, 1981.

12. T. Yoshida and K. Baba, “Dynamic Response of Dams”, Proc. 3rd World Conf. Earthquake Eng., Auckland, Vol. 2, pp. 748-764 , 1965.

13. G. Oberti and E. Lauletta, “Structural Models for the Study of Dam Earthquake Resistance,” Ninth International Congress on Large Dams, Istanbul, Turkey, Sept 4-8, 1967.

14. Zhou, J., Lin G., Zhu,T., Jefferson, A.D., Williams, F.W. 2000, “Experimental investigations into seismic failure of large arch dams,” ASCE Journal of Structural Engineering, Vol. 126, No. 8, 2000, pp. 926-935.

15. Mir, R.A. and C.A. Taylor, “An Investigation Into Base Sliding Response of Rigid Concrete Gravity Dams to Dynamic Loading,” Earthquake Engineering and Structural Dynamics, Vol. 25, 79-98 (1996).

16. Payne, T.L., “Shaking Table Study to Investigate Failure Modes of Arch Dams,” 12th Europeon Conference on Earthquake Engineering, Paper Reference 145, Elsevier Science, Ltd., 2002.

17. D.W. Harris, T.L.Payne, and L.K. Nuss, “Comparison of the Nonlinear Behavior of Concrete Arch Dams using Physical and Numerical Models,” Presented at Third US/Japan Workshop on Advanced Research on earthquake Engineering for Dams, San Diego, CA., June 22-23, Hosted by US Army Corps of Engineers, ERDC, 2002.

18. R. M. McCafferty, “Test Facilities USBR Vibration Test System,” Shock and Vibration Bulletin, Bulletin 41, p. 109-117, December 1970.

19. Harris, David W., C. E. Mohorovic, and T. P. Dolen, “Dynamic Properties of Mass Concrete Obtained From Dam Cores,” ACI Materials Journal, Vol. 97, No. 3, American Concrete Institute, 2000.

20. Harris, D.W., T.P. Dolen, C.E. Mohorovic, and P. Mitchell, “ Properties Obtained from Dam Cores,” Presented at Third US/Japan Workshop on Advanced Research on earthquake Engineering for Dams, San Diego, CA., June 22-23, Hosted by US Army Corps of Engineers, ERDC, 2002.

21. Annual Book of ASTM Stanadards, 1998, V. 4.02, Concrete and Aggregates, American Society of Testing and Materials, West Conshohocken, Pa., 1998.

22. U.S. Department of Interior, Concrete Manual 8th ed., United States Government Printing Office, 1988.

23. Harris, David W., Nathan Snorteland, Timothy Dolen, and Fred Travers, “Shaking Table 2-D Models of a Concrete Gravity Dam,” Earthquake Engineering and Structural Dynamics 2000; 29: 769-787.

24. Bishoff, P.H. and S.H Perry, “Compressive Behavior of Concrete at High Strain Rates,” Materials and Structures, V. 24, pp. 425-450, 1991.

25. Ross, C.A., Kuennen, S.Y., Tedesco, J.W., “Effects of Strain Rate on Concrete Strength,” Session on Concrete Research in the Federal Government, ACI Spring Convention, Washington, D.C., March 1992.

26. Lin, J.I., DYNA3D: A Nonlinear, Explicit, Three Dimensional Finite Element Code for Solid and Steuctural Mechanics: User Manual, Methods Develpment Group, Lawrence Livermore National Laboratory, p. 2002.

Table 1 - Models with associated properties.

Model	Type	Date	Age	Avg Comp	Avg Split	Avg Beam	E	Failure Acceleration, g	
			(days)	(lb./in.^{2})	(lb./in.^{2})	(lb./in.^{2})		Initial Crack	Final Failure
M-1	Monolith - Stripping crack	3/12/99	7	28.1		3.2			
M-2	Monolith	3/31/99	7	23.25		4	2302.6	.75	5.0
M-4	Monolith - 1st Pulse	7/28/99	6	33.64			3761		
M-5	Monolith - 1st Pulse	8/12/99	6	37.5	4.83	3.1	3088.4		
M-6	Vertical Joint (saloon door)	8/27/99	7	25.6	4.67			0.7	0.85
M-7	Vertical Joint	5/2/00	8	40.3				1.5	1.5
M-8	Vertical Joint	6/21/00	7	28.2				1.5	1.5
M-9	Horizontal Joint	7/19/00	7	36				0.95	1.75
M-10	Horizontal Joint	8/2/00	7	52.1			5172.1	1.65	1.65
M-11	Vertical Joint	8/22/00	6	41.97	4.4		3758.8	1.2	1.2
M-12	17 Vertical Joints	10/3/00	5	27.01			2146.6	0.6	0.6
M-13	17 Vertical Joints	4/10/01	5	23.2	3.58		3461.5	0.5	0.5
M-14	2 Horizontal, 17 Vertical Joints	4/24/01	5	19.625	3.09		3099	1	1.25
M-15	2 Horizontal, 17 Vertical Joints	5/1/01	5	21.4	4.05		3948	0.75	0.75

Table 2 - Comparison of Model Mix Properties and Properties Measured from Dam Cores

Property	Properties Measured from Dam Core or Dam		Model Value		Similitude Ratio
	Minimum	Maximum	Measured	Scaled by 150	
Failure Mechanism Shear angle in Compression		65	65	na	1.0
Tension Strength (psi)	215	785	4.1	615	1.0
Frequency Input Field Shake tests - Periods First Period of quake Model Calculated Periods Input motion	0.13 0.17	0.22 0.28 0.32 0.25	0.07 0.09 0.10 0.072	na	1.0
Strain Rate	approx 1 x 10^{-3}		approx 1.4 x 10-3	na	1.0 to 1.04
Compression Strength (psi)	1400	8400	31	4650	1.0
Young's Modulus(psi)	750,000	7,500,000	3415	525,000	0.7
Density(lb/ft**3)	141	157	118	na	0.85

Table 3 - Model Concrete mix components.

Component	Lab Mix lb./yd.^{3}	Volume in mix
Air		0.14 (1/2% entrapped air assumed)
Water	739.8	11.86
Cement	156.6	0.8
Bentonite	63	0.39
Sand	2245.41	13.81

Note: water/cement = 4.72 Bentonite/(Bentonite+Cement)= 28.7%

Figure 1 - Failure of Modeled Material and 50 Year recovered Core

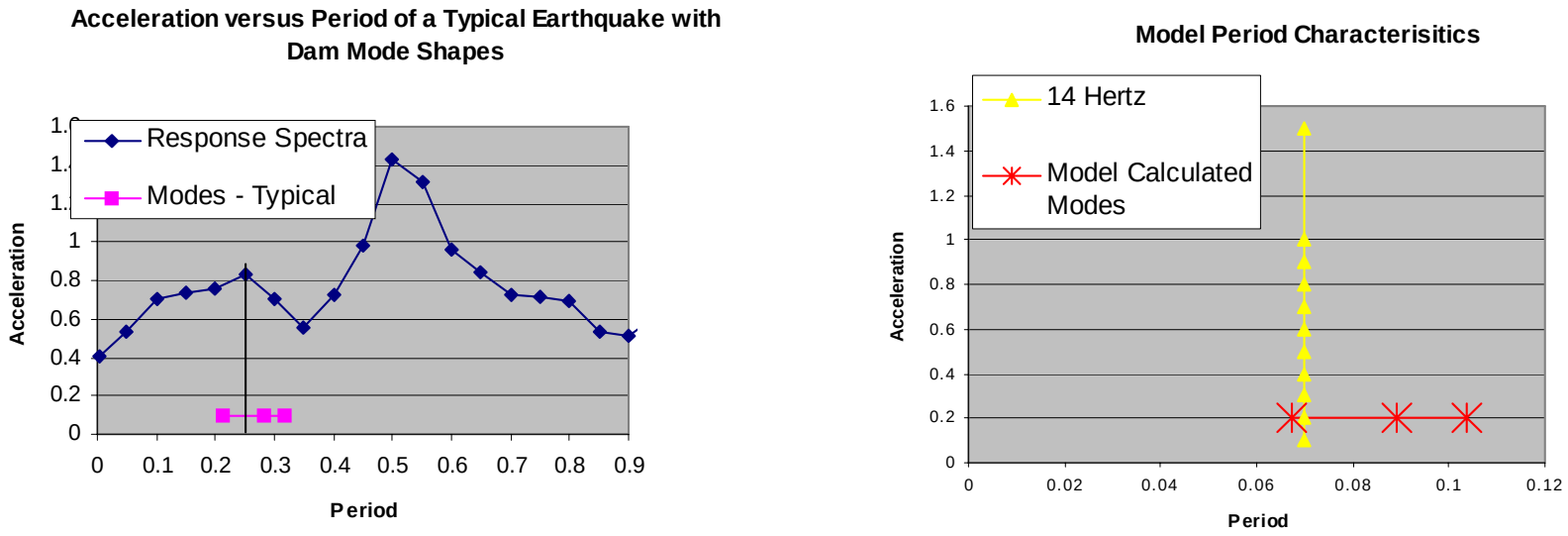

Figure 2 - a. Response spectra and 3 mode shapes measured on a typical dam b. Calculated mode shapes and model input motion

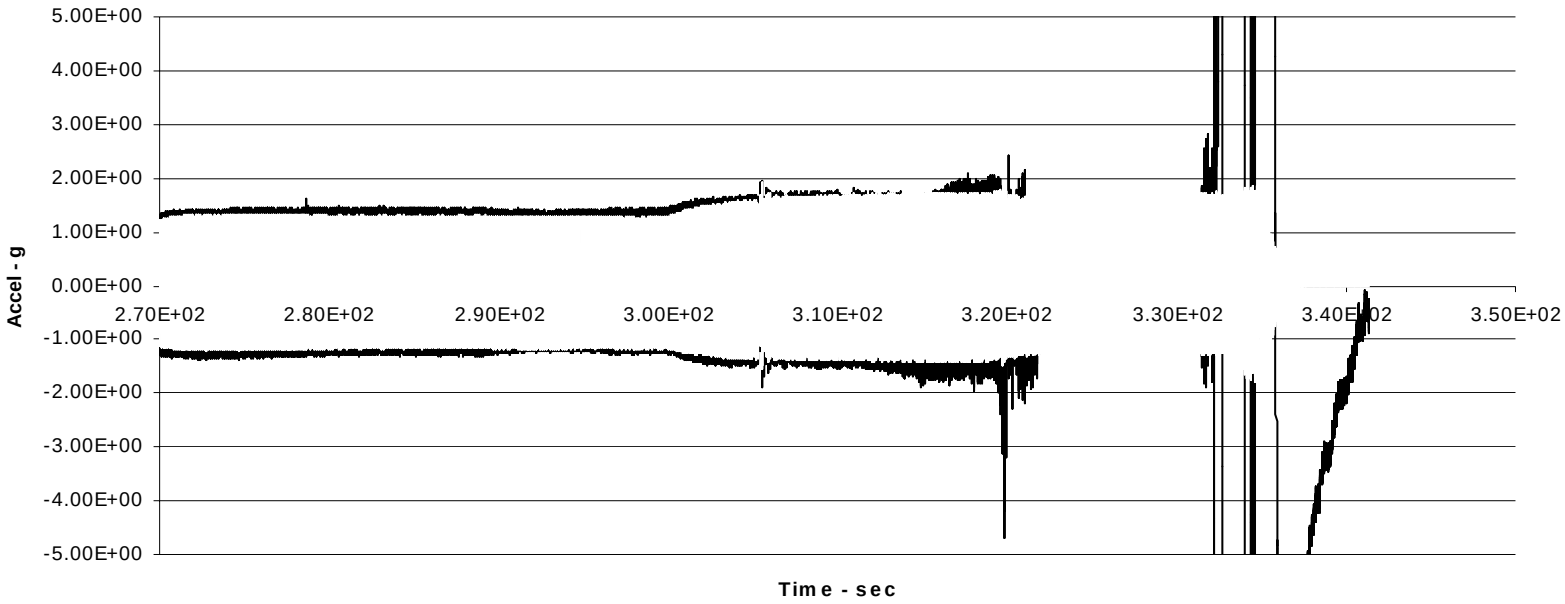

Figure 3 - Instrumentation data for Horizontal Joint Model Base (White) and 3/4 Height (Black) accelerometer

Figure 4 - Shake table model ready for testing, note reservoir behind dam (covered in plastic)

Figure 5 Model with joints following failure

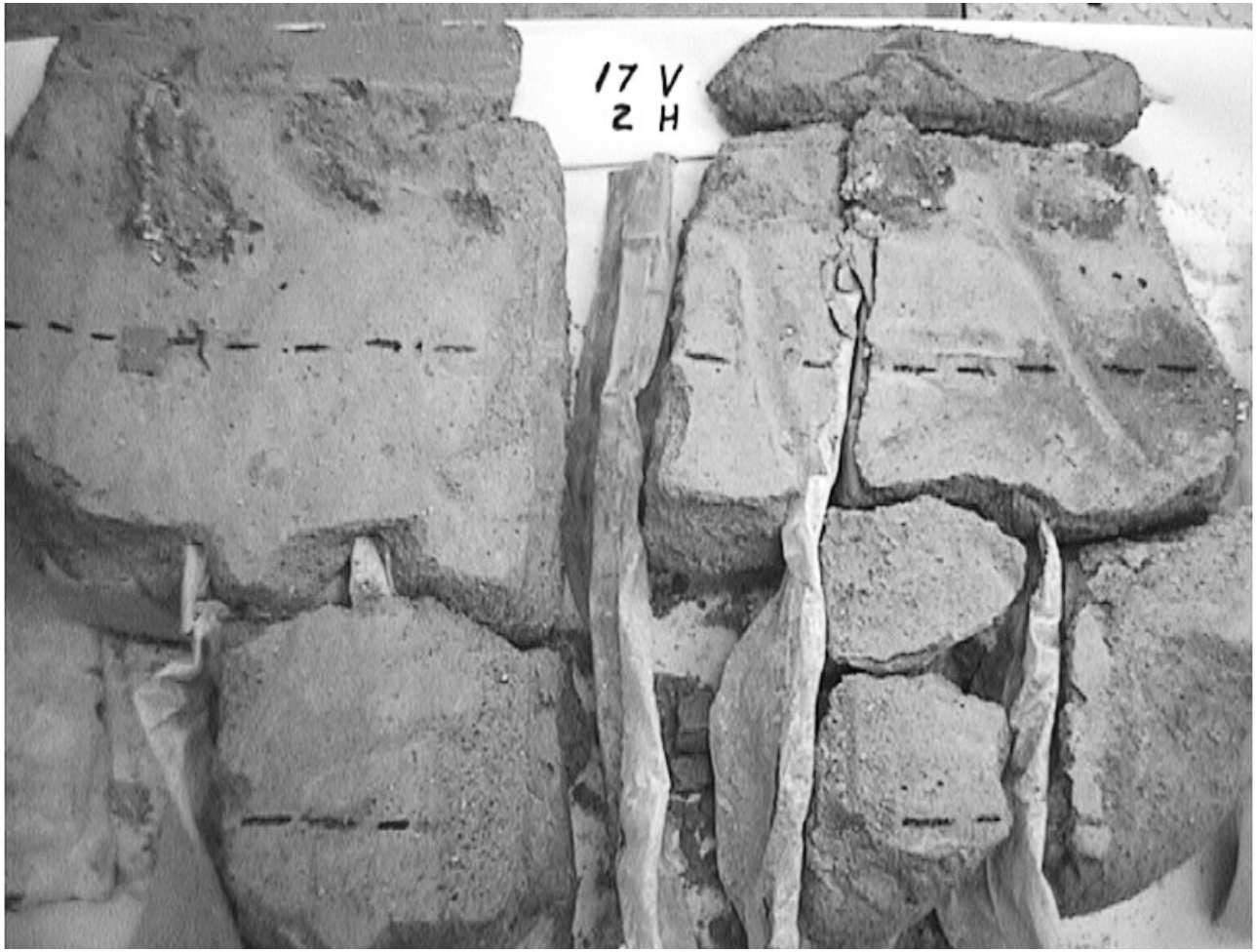

Figure 5 - Illustration of initial cracks in models

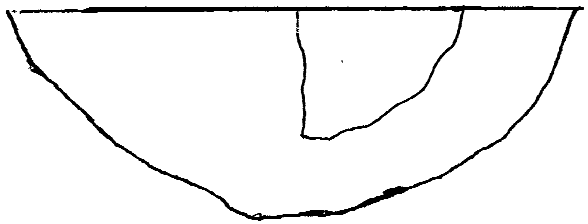

Figure 5a. Initial crack of monolithic model

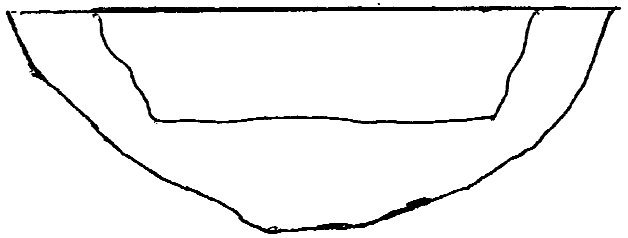

Figure 5b. Initial crack of horizontal model

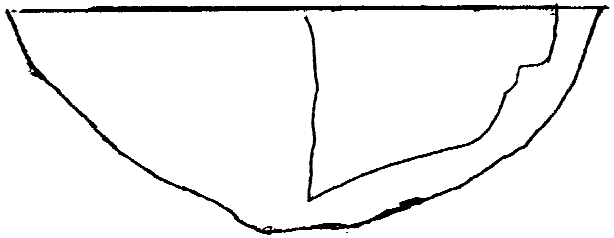

Figure 5c. Initial crack of vertical joint model

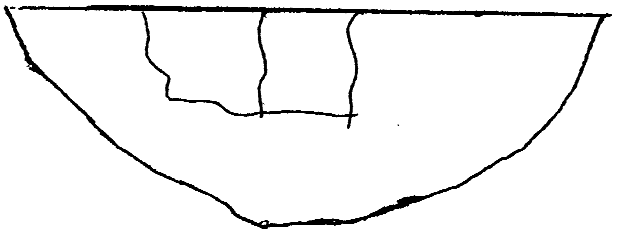

Figure 5d Initial crack of 17 vertical, 2 horizontal joint model

Figure 6 - Final Failure of Models

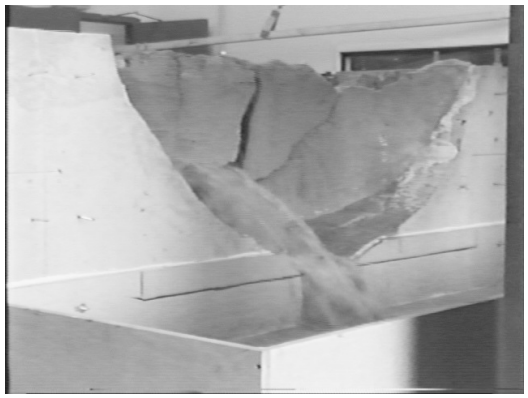

Figure 6a - Monolithic Model

Figure 6b - Horizontal Joint Model

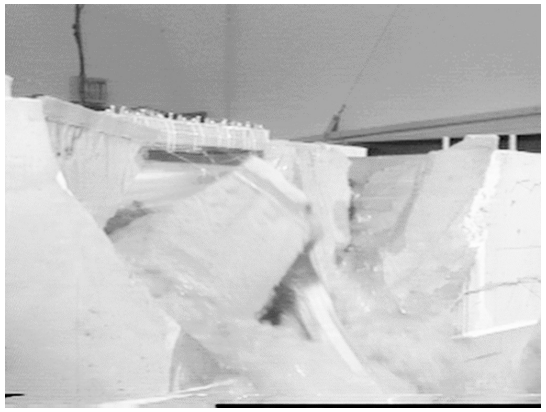

Figure 6c - Vertical joint model

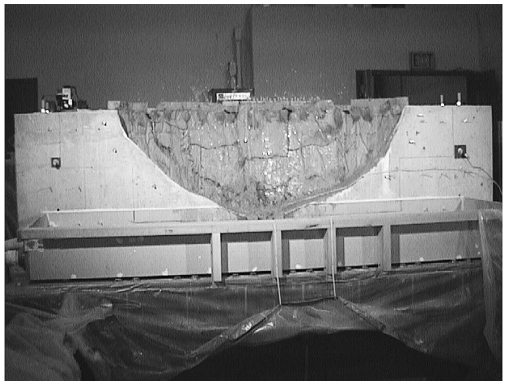

Figure 6d - 17 vertical, 2 horizontal joint model